QCX
Avro
CF105
P-FFM-47

(11)

FILE IN VAULT

UNCLASSIFIED

ANALYZED

CEPE
Armstrong

CONFIDENTIAL P/F.F. MODELS/47

C-105

SUMMARY OF THE FIRST SEVEN FREE FLIGHT MODEL TESTS & RESULTS

AUGUST 1957

COPY # 11

AVRO AIRCRAFT LIMITED

UNCLASSIFIED

CONFIDENTIAL

AVRO AIRCRAFT LIMITED
MALTON - ONTARIO
TECHNICAL DEPARTMENT

AIRCRAFT: C-105		REPORT NO. P/F.F.M./47	SHEET NO. (i)
		PREPARED BY: D. Ewart & W. Taylor	DATE: July 1957
		CHECKED BY:	DATE:

C-105

FREE FLIGHT MODELS

Summary

An account is presented of work done in connection with the Free Flight Model programme, for models up to and including Number 7. This includes the purpose of the programme, preliminary work both theoretical and practical, a brief history of the tests, the relevant configurations and reduced test data. The report concludes with some suggestions for future Free Flight Model work.

INDEX

	Sheet
Summary	(i)
Notation	(iv)
Aim of the Free Flight Tests	1
General Preliminary Work	2
The Free Flight Model Programme	4A
The First Seven Models	7
Results	21
Conclusions and Suggestions for Future Free Flight Model Work	25
Appendix "A" Drag Corrections	27
References	29

Tables	Table
Model Weights and Inertias	I
Instantaneous Drag; Model #5	II

Figures	Figure
Static test of "Nike" booster motor, & comparisons	1
Typical model trajectory - Model #7	2
Typical test meteorological data - Model #7	3
Typical telemetered data - Model #7	4
Typical telemetered data (contd.) - Model #7	5
Comparison of D.T.T.V. #2 velocity, from doppler and kines.	6
Mach No. vs. time Model #1	7
" " " " Model #2	8
" " " " Model #4	9
" " " " Model #5	10
" " " " Model #6	11
" " " " Model #7	12
Comparison of Mach No. from four sources Model #6	13
Comparison of Mach No. from four sources Model #7	14
Dynamic Pressure vs. time Model #1	15
" " " " Model #2	16
" " " " Model #4	17
" " " " Model #5	18
" " " " Model #6	19
" " " " Model #7	20
Drag Coefficient vs. Mach No. Models #1 & 2	21
" " " " " Model #5	22
" " " " " Model #6	23
" " " " " Model #7	24

Figures (Continued) Figure

Calibration of Probe Static, Models #6, 7, 8, & 9 25

Comparison of C_{n_β} vs. Mach No. Models #4, 5, 6, 7 with 8 & 9 26

Mean Reynolds Number of Free Flight Tests 26A

Diagram of Crude Free Flight Model 27

G.A. of Free Flight Model & Booster 28

Overlay Drawing of Model #5 29

" " " Model #6 30

" " " Model #7 31

Basic C-105 Configuration 32

Airborne & Ground Telemetery Systems & Tracking Radar System. - Block Diagrams. 33

C-105 Free Flight Model - Structural Breakdown 34

Commutated Duct Pressure System - Drag Models 35

Model telemetery equipment 36

Marry - up of Commutated Press. System 37

Angle of Attack & Sideslip Vane 38

Model & Booster Launcher 39

Model #1 on launcher 40

Model #5 on launcher 41

Model #6 on launcher 42

Model #7 on launcher 43

Model #7 - instant after launch 44

Model #7 - instant after separation of model from booster 45

Doppler Velocimeter Radar Antennae - Picton 46

Tracking Radar Display - Picton 47

Avro Mobile Telemetery Ground Station 48

Range Control Room, Picton 49

NOTATION

α	incidence, degrees
β	angle of sideslip, degrees
δ_e	elevator deflection, degrees
R	Reynolds Number
M	Mach Number
a	speed of sound, ft/sec.
q	free stream dynamic pressure, $= \frac{1}{2}\rho V^2$, lb/sq.ft.
ρ	air density, slugs/cu.ft.
h	altitude, ft.
V	free stream velocity, ft./sec.
b	span, ft.
$\bar{c}$	mean aerodynamic chord, ft.
S	wing area, sq.ft.
W	model weight, lb.
m	model mass $= \frac{W}{g}$, slugs
g	acceleration due to gravity, ft./sec.^{2}
k_x	roll radius of gyration, ft.
k_y	pitch radius of gyration, ft.
k_z	yaw radius of gyration, ft.
I_x	roll moment of inertia, $m.k_x^2$, slugs ft.^{2}
I_y	pitch moment of inertia, $m.k_y^2$, slugs ft.^{2}

I_z yaw moment of inertia, $m.k_z^2$, slugs ft.^{2}

$\mu_1 = \frac{m}{\rho S \bar{c}}$

$\mu_2 = \frac{m}{\rho S b}$

η angle between principal axis and body OX - axis, degs

A axial force in direction XO, lb.

Z normal force in direction OZ, lb.

D drag force, along wind axis, lb.

L lift force, normal to wind axis, lb.

N yawing moment, about OZ axis, lb.ft.

M pitching moment, about OY axis, lb.ft.

$C_D = \frac{D}{qS}$

$C_L = \frac{L}{qS}$

$C_n = \frac{N}{qSb}$

$Cm = \frac{M}{qS\bar{c}}$

$C_{n_\beta} = \partial C_n / \partial \beta$

$Cm_\alpha = \partial C_m / \partial \alpha$

P period of oscillation, secs.

$T_{\frac{1}{2}}$ time to damp to half amplitude, secs.

Subscripts:

m - free flight model C-105

A - full scale C-105

Diagram of axes in Ref. 75

Aim of the Free Flight Tests

The original purpose of the Free Flight Model tests was to provide dynamic stability and control data for the C-105 in the pitching plane, and dynamic stability data in the yawing and rolling planes. Model speed would cover most of the C-105 supersonic and transonic speed range, while the model, with dimensions and inertias to scale, would be free to move in all planes.

Design and manufacturing difficulties in the elevator operating system delayed the completion of the longitudinal stability models, while the mechanism to produce the yawing disturbance in the directional stability models had yet to be proven in a crude model. In the meantime it was decided to go ahead with another phase of the programme, that of determining aircraft drag from free flight model tests.

Up to this time the only experimental data available on drag for the C-105 was from Wind Tunnel tests, with the models, both .03 and .04 scale, mounted on a "sting". There are several possible causes of inaccuracy in tunnel measurement of drag; the effect of the "sting", relatively low Reynolds Number of test, and the difficulty of making an accurate strain gauge drag balance free from interaction of the other components.

A more accurate assessment of C-105 drag was possible from free flight tests, because of freedom from interference, much higher Reynolds Number and more reliable means of drag measurement. The effects upon aircraft drag of two "Area Rule" modifications to the fuselage and canopy contours, were also investigated in this series of free flight tests.

The decision to embark on a series of free flight tests using C-105 models was made in the middle of 1953. A ground launch method was chosen, in which the model is accelerated up to flight speed by a booster rocket before separation of the booster. While in free flight, subsequent behaviour of the model is determined from data radioed, or telemetered, down to a ground station from equipment contained in the model.

Choice of the ground launch technique was made in preference to other methods, such as air launch from an aircraft, or testing in a ballistic range. In ballistic tests, an elegantly simple system of obtaining early design data, a very small scale model of the aircraft is fired from a large calibre gun; however, the model usually carries no instrumentation, accuracy is limited and speed range restricted. Air launching utilizes gravity force to accelerate the model, so that maximum speed is usually limited. Even if the model is rocket boosted, control and measurement of trajectory and speed is difficult. Using a ground launch, speed and trajectory may be carefully controlled & measured, while accurate telemetry measurements are made easier.

This report is concerned with only the first seven models, the first four being "Crude" models and the last three being representative or "Drag" models. Subsequent models were to be disturbed while in free flight, in the directional and pitch planes, to ascertain the stability both laterally and longitudinally.

General Preliminary Work

After an assessment of the data to be telemetered from the model while in flight, and the internal space therefore required for the appropriate instrumentation and electronics, and also in order to obtain the greatest test Reynolds Number, a model scale of one-eighth full size was decided upon.

Various booster motors and combinations of booster motors were considered, the one used being a "Nike" booster (JA TO XM5) of approximately 45,000 pounds thrust, and 150,000 lb. sec. impulse (See Fig. 1)

"Drag" separation of booster rocket and model was decided upon in preference to the "Explosive Bolt" technique as used by C.A.R.D.E. In this drag separation method, developed by the Pilotless Aircraft Research Division of N.A.C.A., the greater drag/weight ratio of the booster when the boost stage is finished slows the booster more rapidly than the model, and the two separate owing to the differing decellerations.

Booster horizontal tail was designed to maintain a good static margin of model booster combination at all speeds. (See Ref. 58 & 63 and Table I)

The model booster combination was checked for elastic divergence (Ref. 63, 64) and for flutter of model (Ref. 21) and model booster combination (Refs 16, 22). Effects of manufacturing inaccuracies of model and booster on their flight were also checked. (Ref. 23, 61) References 15, 16, 18-20, 24-31, 51-56 cover the design of model and booster, and the "zero - length" launcher, together with the tests for model distortion under simulated air loads, and the measurement of model and booster weights and inertias.

Data reduction techniques were investigated, (Ref. 2), later to be applied to actual tests (Ref. 9).

Free flight models were equipped with an FM/FM telemetering system utilising standard R.D.B. channels. The baeic elements of the airborne eyetem are ae in Fig. 33

Selection of theee elements wae made after exhaustive environmental tests of various types and makes. Transducers fell into the following electrical categories; Inductive, Potentiometer and Strain Gauge Bridge (almost entirely unbonded), and were used to make measurements of pressures, and linear and angular accelerations.

The principle of operation was euch that a change of the quantity being measured rssulted in an equivalent electrical shift in the traneducer causing a shift in the subcarrier, (an audio frequency). This resulting frequency modulates the tranemitter (ueing a carrier frequency of 218 or 224 mc/e.) which in turn sende its signal via the transmitter to the ground station (Refe. 3, 5, 6, and 11)

One of the more delicate instrumente, the "$\alpha - \beta$" vane, to measure angle of attack and sideelip of the model in flight, was an electrically modified vereion of the N.A.C.A. design and required careful testing (Ref. 13). Later, an attempt wae made to measure etatic preseure with a probe, attached to the front of the $\alpha - \beta$ vane (Ref. 10) (See Fig. 38)

Fig. 34 is an "exploded" view of the model structure, and indicates the breakdown into sub components for manufacture. Model depicted is a longitudinal stability model; drag models differed only in having fixed elevators.

During model construction, considerable difficulty was experienced in the manufacture of accurately profiled wings for the scale models for drag end stability tests. Initial efforts to cast them in aluminum alloy were unsuccessful owing to warping of the castings, and efforts to correct the warp mechanically, failed. Machining the wing from cast billets of magnesium alloy also proved unsatisfactory, and the model wings were finally machined from rolled billets of magnesium alloy. As an interim measure, for model #5 a composite fabricated wing was used.

The commutated duct pressure measurement system of fig. 35, as used on all the drag models, does not show the transducers, which convert the sensed air pressure into an electrical signal.

With a power of 2 watts each, the two transmitters operate on 218 m.c. and 224 m.c. carrier frequencies, and are modulated by audio frequency sub-carrier oscillators, which in turn take their signals from associated transducers. The coupler, an impedance matching device, allows the two transmitters to use the one ½ wave length slot antenna.

Power supply is from silver peroxide-zinc lightweight batteries, activated by potassium hyroxide solution (Ref. 8). Output is 6 volts at 10 amp. on the low tension portion, with a life of approximately 1 hour. In addition nominal voltages of 108, 180,28 and reference 5 volts are provided.

Shown in Fig. 33 is a block diagram of the telemetery ground station, while Fig. 48 shows the station interior. With the model on the launcher, the "launch" frequencies of the various data channels are noted, and a five point frequency calibration is recorded on the tape. Calibrations are repeated at the end of the test.

Placed in pack form below its location in the model is the commutated pressure system (Fig. 37). α - β vane, with static probe, as in Fig. 38, was maintained in the zero deflection position by a cylindrical jig (Figs 40 to 43) which also served as protection. This was removed just before firing.

Free Flight Model Programme

During the programme an attempt was made to keep up to date with design changes. For the "Drag" models the configuration changes may be noted from Figs. 29 to 31 , which are exact transparent overlays upon the basic configuration of the full scale C-105 in Fig. 32 Crude models took the form shown in Fig. 27

CONFIDENTIAL

AVRO AIRCRAFT LIMITED
MALTON - ONTARIO
TECHNICAL DEPARTMENT

REPORT NO.	P/F.F.M./47
SHEET NO.	5
AIRCRAFT:	C-105
PREPARED BY	W. Taylor & D. Ewart
DATE	July 1957
CHECKED BY	
DATE	

SERIAL	MODEL DATA
1 & 2	Crude representation. C.G. at .25 MAC Approx. scale radii of gyration. Slab wing, profilsd fin. Telemstsry on 5 channsls. No intaks ducts.
3 & 4	As for ssrials 1 & 2 but with yaw impulss mechanism installsd and full telemstsry.
5	Accurate Scals model. C.G. at 0.25 MAC. Plain leading edge with 8% notch. 50° conical radar noss shape. J-67 intakes and ducts. Intermediats J-75 rear fuselage. Fixed control surfaces.
6	Accurats scale model. C.G. at 0.25 MAC. Drooped leading edge with 5% notch and 10% sxtsnsion outboard of notch. 30° conical radar nose shaps. J-75 intakss, ducts and rear fuselage. Pressure rakes in ducts. Partial area-ruling of fusslags. Fixed control surfacss.
7	Accurats scals modsl. C.G. at 0.25 MAC. Droopsd leading sdgs with 5% notch and 10% sxtsnsion outboard of notch. 30° conical radar noss.

7 (Continued) J-75 intakes, ducts and rear fuselage. Pressure rakes in ducts. Special area ruling. Fixed control surfaces.

All models were to 1/8 th scale with the exception of the fins, which were made oversize to ensure model stability.

The wings of models 5, 6, and 7 had 0.75% negative camber, as on full scale.

Models 8 and 9 were lateral stability models; 10 and 11 were longitudinal stability models. These will be covered fully in report. P/F.F.M./48. (Ref. 72)

Models 1 to 5 and 8 to 11 were fired at the Point Petre Range of the Canadian Armament, Research and Development Establishment (C.A.R.D.E.), near Picton, Ontario. Models 6 and 7 were fired at the Wallops Island Range of the N.A.C.A. Pilotless Aircraft Research Division (P.A.R.D.), in Virginia, U.S.A.

All the models were launched from mobile "zero - length" launchers, placed on a concrete firing ramp.

At Picton there were several kine theodolites dispersed around the range, manually operated to track the model in flight. From the data of two or more kines could be obtained the trajectory and approximate space velocity of the model. There was also a modified S.C.R. 584 tracking radar located quite near to the firing site, which could provide a trajectory of the model in flight. Aerodynamic data from the model was telemetered to an Avro mobile ground station and to the C.A.R.D.E. ground station, where it was recorded on magnetic tape for later playback.

A common time base was provided by the pulse which triggered the synchronised kine shutters each .2 sec., these kine pulses being recorded on the magnetic tape along with telemetered data.

Meteoroligical data was obtained from a radiosonde balloon, tracked through its ascent by the tracking radar.

In general the N.A.C.A. range at Wallops Island was similar to that at Picton, but without the kine theodolites, and employing the use of doppler velocimeter radar to measure model speed. Trajectory was established from tracking radar data, and was used to correct the doppler velocity. As at Picton, meteorological data came from a radiosonde balloon released immediately after the firing and tracked by radar through its flight path. At Wallops, owing to an incompatible telemetering system, telemetered data was recorded only by the Avro ground station.

The first seven models.

It was originally intended that the models should obtain speeds in the region of Mach 2, but increases in both model and booster weight, as the design progressed, produced a final separation Mach number of 1.7.

At such speeds the directional stability with the full scale vertical tail could have been marginal, and it was decided to use a tail with 50% more area than a corresponding model tail based on the full scale aircraft. In addition, the model centre of gravity was located by ballasting at 25% of the mean aerodynamic chord to give further insurance of directional stability and at the same time provide ample margin of longitudinal stability.

In order to produce the minimum disturbance at separation, the model elevators were set at approximately the trim angle for the separating speed. (Ref. 76)

The first four models were relatively "Crude" models, an approximate representation of the C-105 model having a rectangular section fuselage with parallel sides, a const. dia. sting at the forward end and blunt base at the rear end. With the correct shape in planform as the original C-105, that is a plain leading edge, the wing in section was a blunt double wedge with flat top and bottom. This was fabricated from a composite core of plywood and masonite sheathed with steel plates, the whole bonded together and rivetted. The fin of correct aerodynamic shape, was used on all subsequent free flight models.

Crude model radii of gyration were maintained fairly close to equivalent full scale values and with similar relation to each other. (See table I).

(a) Free Flight Model #1

Fired on 14 December, 1954 (Ref. 1). The purpose of the test was to evaluate the techniques for launching, separation, telemetering and tracking, also the structural, dynamic and aerodynamic qualities of the booster model combination. (Fig. 40)

Being the first test in the series, there were many unknowns.

The launcher mechanism operated well, while estimates of clearance between booster tail and launcher during launch were confirmed. Damage to the launcher from rocket blast was insignificant, but a more positive means of anchoring the launcher was found necessary. Also checked were freedom from elastic divergence and from flutter of the model booster combination, trajectory, during boost and the amount of roll during boost from manufacturing inaccuracies.

Separation was found to be clean and rapid, with separation "kicks" of no more than ±10g normal nor ±5g transverse, accelerations. This typical separation pattern also indicated that shielding of the telemetering antenna by the booster body was not a problem and signal strength was more than adequate over the whole flight. The operator of kine theodolite #1, located behind the line of fire experienced some distraction from the booster during separation, while tracking radar followed the booster instead of the model. Subsequent booster trajectory proved to be safe.

After separation, it was intended to determine the trajectory from kine theodolite and tracking radar data, but, as noted, tracking radar followed the booster while kine operators failed to follow the model for more than 1 second. However, this almost zero lift trajectory was observed visually and confirmed by telemetery records of the "splash" time, showing the trajectory to be safe. An idea was obtained of the flight time in the useful speed range, and of the drag of this 1st. crude model.

In the absence of data from kine theodolites and and tracking radar, the model "space" velocity was obtained from integration of the longitudinal accelerometers, allowing for the decelerating effect of gravity, and corrected to air velocity by allowing for wind velocity. After the firing a radiosonde balloon had been released; as it rose the ambient air temperature and pressure were telemetered back to the ground station. At the same time it was being followed automatically by tracking radar, to provide balloon height and wind velocity at this height.

One useful feature of the "kick" at separation was that it provided a disturbance in pitch and yaw, and from the subsequent oscillations it was possible to measure the period and damping in pitch and yaw, on the recorded traces of telemetered data.

These crude model firings served to check the functioning of the following accelerometers and instrumentation, and of telemetering to the ground station. They also assisted in the choice of transducer ranges for future models.

Free Flight Model #1 instrumentation.

- Boost accelerometer
- Drag accelerometer
- Transverse accelerometer
- Normal accelerometer
- Pitch angular accelerometer
- Separation indicator

The normal accelerometer failed to operate on model #1 but gave good data on model #2. Both C.A.R.D.E. and Avro ground stations obtained good records of the telemetered data on magnetic tape, and this was given to Bell Aircraft, New York, U.S.A., to reduce to aerodynamic functions. The data was also reduced by hand at Avro, to check the Bell results. (Refs. 32 & 60)

From the "kick" at separation was obtained the frequency and damping in both pitch and yaw, at the separation speed, and typical maximum values of the measured functions experienced by the model at separation.

(b) Free Flight Model #2

Fired on 16 December 1954. (Ref. 1) This model was fired to confirm the success of F.F.M. #1 in all the aspects under investigation. Instrumentation was asmodel #1.

Before firings of both models 1 and 2 kine operators were provided tracking practice with a 5" H.V.A.R. test tracking vehicle (T.T.V.), fired at the same launch angle of the C -105 model, and attaining approximately the same speed. However, the T.T.V. did not provide the same distraction of model and booster separating, and on model #2 as on model #1, kine theodolites failed to track the model in free flight for more than 1 second. Model air velocity was again found by integration of drag and boost accelerometer readings, allowing for model inclination, and correcting for wind velocity. As with model #1, all aspects of the launch and flight checked well; all instruments functioned correctly and telemetery was good. (Refs. 33 and 60)

(c) Free Flight Model #3

Fired 12 May, 1955.

This was a crude model, fired with the object of testing the yaw impulse mechanism. To provide disturbances in yaw a mechanism was designed to fire small charges from a hole on either side of the model nose, timed and indexed to fire once every second. Originally intended to produce a 10 lb.-sec. impulse, tests showed the charges to give approximately 7.8 lb.-sec. on a moment arm of approximately 4 ft. (Ref. 4)

Also confirmed were the performance during launch, boost flight and separation of models 1 and 2, the subsequent model trajectory, and the instrumentation and telemetery.

Instrumentation:-

Pitot pressure
Boost accelerometer
Transverse accelerometer
Normal accelerometer
Drag accelerometer

Yaw angular accelerometer
Roll rate
Instrument bay temperature
Temperature at sting
Angle of attack α
Angle of sideslip β
Static pressure (on probe)
Static pressure (behind compensator cone)

As the list indicates, several new instrument systems were tested on model 3. A pitot tube was located on an arm below the fuselage. (Positioned as in Fig. 28) There was considerable position error in this location, but had all other means of speed measurement failed on later models, this pitot, with calibration, would have given a close approximation to the actual speed. Instrument bay temperature proved to be nearly constant over the useful portion of the model trajectory. Sting temperature in the region of the α-β vane showed a rise from 50°F to 95°F, with considerable lag, as speed increased.

Mention was made earlier of the α-β vane; model #3 was the first on which this vane was used, and the vane appeared to function correctly.

Failure in the drive between motor and indexing mechanism was the most likely reason why the yaw impulse mechanism failed to operate. Subsequent modification of this drive rectified the trouble. However, adequate "kick" was obtained at separation to give a disturbance in yaw, and readings on all instruments.

Static pressure was measured at two positions on the nose probe carrying the α-β vane, one of these being behind a cone-like compensator as used in some N.A.C.A. tests. Neither static pressure source was found to be reliable. The remaining instruments appeared to give good data.

For this model the data was reduced at Bell Aircraft from the Avro tape recording. Due to pressure of work & malfunction of the yaw mechanism no further work was done on this model test.

Kine theodolites tracked reliably over less than 7 secs. of flight. Radar failed to track the model.

(d) Free Flight Model #4

Fired 14 June, 1955

The yaw impulse mechanism was modified to overcome the trouble encountered on model 3, and tested on model 4, which was instrumented as model 3 but without any temperature or pressure measurement, (Refs. 7 and 35).

This time the yaw impulse mechanism functioned perfectly, providing sideslip angles of up to $\pm 2^{\circ}$ within the first 20 secs. of flight. There was only a slight disturbance in pitch at each impulse, sufficiently small to ignore the effect of pitching motion upon the general equations of motion, and yet adequate to provide a measure of the frequency in pitch.

All instrumentation and telemetery functioned correctly, including the α - β vane. (Ref. 35)

Kine theodolites, assisted by the puffs of smoke from the yaw impulse changes, followed the model for about 23 secs. Tracking radar performance was again inadequate.

Model speed was obtained from the kine theodolite data, corrected for wind velocity as determined from radiosonde balloon.

Preliminary values were obtained for stability in sideslip (C_{n_β}). (See Figure 26).

Due to some inaccuracies in the reduction of the previous model (model #5) data at Bell, data reduction was performed at C.A.R.D.E., Valqartier, P.Q., by Avro personnel using C.A.R.D.E. equipment.

All instrumentation and telemetery functioned well. Some idea was obtained of the effect of yaw impulses on the trajectory of the model, and the estimated peak values of sideslip (Ref. 4); peak values of transverse acceleration and yaw angular acceleration were also assessed, and it was confirmed that there was very little disturbance in pitch from the yaw impulses. The effect of this damped yawing motion on drag was negligible.

(e) Free Flight Model #5

Fired 14 May, 1955 (Ref. 7) (Fig. 41)

An accurate 1/8th scale model of the C-105, this model incorporated all the design features which had been finalised at the time of model construction (See Fig. 29). Basically, this had a $3\frac{1}{2}$% thick wing with a "notch" on the leading edge at the transport joint, 8% of local chord. There were no leading edge extensions nor "droop", nor was there any "area rule" applied to the fuselage. Intakes were as designed to take the J-67, rear end was modified as for J-75. The radome had a nose angle of 50°.

The main purpose of the test was to determine from velocity data and telemetered data the supersonic drag coefficient of the C-105.

Also unknown was the stability of the model above M = 1.2. The test confirmed estimates of trajectory, separation forces and the steady roll due to manufacturing inaccuracies.

Instrumentation was as follows:

Boost accelerometer
Drag "
Normal "
Transverse "
Pitot pressure
Static pressure
Angle of attack α
Angle of sideslip β
Separation
Static "Buzz"
Base pressure
Pitot "Rake" at duct exit.

In addition there were two subcarrier channels each commutated to give data from 12 pressure points around and in the ducts, totalling 24 pressure points. Up to that time this was the greatest amount of instrumentation even to have been put in a free flight rocket model.

Kine theodolites gave trajectory data over the first 6 secs. of trajectory, after this there was only one kine operator following the model.

Tracking radar locked on at 13 secs. with the "boresight" camera corrections, and tracked the model for the remainder of the flight. This left the trajectory between 6 and 13 secs. to be interpolated.

Kine theodolite data was read from the films, corrected for collimation and tracking error, and with each kine giving a "skew" line in space, the model was assumed to be at a point from which the sum of the squares of perpendiculars to the skew lines was a minimum. Kine cameras were synchronised with a master timing unit to take pictures at 5 frames per sec. Utilising an 1.B.M. digital computer, the model trajectory was obtained, in rectangular coordinate form, also the model velocity, which was based on space distance travelled in .2 sec. intervals. To assist tracking the model and to give contrast on the film, the model was painted dayglow red.

Meteorological data was obtained as before, by releasing a radiosonde balloon immediately after the firing.

Bell Aircraft reduction of the Avro tape was found to differ considerably from C.A.R.D.E. tape reduction by Avro personnel at Valqartier, P.Q., Subsequent checking at Avro showed that there was negligible difference between the two tapes. After considerable hand checking, the data from Avro reduction was used in all further analyses.

In the absence of any velocity data from kine theodolites after 6 secs., the kine separation velocity was used as a basis, and subsequent model space velocity, obtained by integrating longitudinal accelerometer readings, corrected for gravity component. Wind velocity was a further correction to give final air velocity. Drag accelerometer and normal accelerometer readings were combined vectorially to give the true drag along a wind axis. Several corrections were made to this drag value to allow for differences between configuration, and conditions of model and full scale. (See Appendix A) For correction of duct mass flow to full scale the commutated pitot and static pressures in the aft part of both ducts were used. Presence of rapidly

UNCLASSIFIED

fluctuating pressures in the intakas was to ba detected by the static "buzz" pressure point.

A check on the speed was obtained from the pitot pressure in combination with radiosode static pressura.

Approximate value of Model C_{N_β} were obtained (Fig. 26) but it was impossible to measure damping. The model experienced a moderata steady state roll, and, due to separation kick, had also periodic roll, yaw and pitch, this motion being divergent for the high ranga of Mach No. (Fig. 4) It appeared from later analysis that this was dua to inartia coupling, as mean α was 1.6° just after separation, and $\eta = 3^\circ\ 47'$ so that the principal axis was tilted down at approximately 2.1°. On the full scale C-105 with tha c.g. at $.2994\bar{c}$ $\eta = 1^\circ\ 42.5'$ or with the c.g. at $.25\bar{c}$ as on the model $\eta \doteq 1^\circ$, so that this unstable condition would not have occurred on the full scale aircraft at the same α.

Subsequent theoratical investigation into model dynamics using estimated derivatives in the Boeing Analog Computer with 5 degrees of freedom (incidence, pitch, sideslip, roll and yaw), showed no such divergence, but with slight modification of the derivatives a divergant motion very similar to that experienced in frea flight was revealed. Subsequant raising of the principal axis to $\eta = 1\frac{1}{2}^\circ$ gave a damped reponsa on the analog computer. This was verified on model #8, in which η was made $1^\circ\ 50'$ by addition of ballast.

Re-evaluation of Picton Ranga

After the first five Fraa Flight Models had been fired it was decided that the Picton range was inadaquata to provide the test coverage of tha order raquired in C-105 firings, and arrangements were made to fire the naxt two models in the U.S.A., whila improvements could be made at Picton.

Tha S.C.R. 584 Tracking Radar at Picton was too close (200 yds.) to "lock-on" to the model prior to launch when using a baacon in the model. The incorporation of a delay circuit into the beacon to artificially increase the modal to tracking radar distance by an additional 1000 yds.

contributed to erratic triggering of the beacon transmitter. Several types and locations of beacon were tried in experiments to improve radar tracking and reliability. One of the main difficulties was that when "skin" tracking, the signal reflection from the booster dwarfed that from the model just after separation, with consequent difficulty in tracking the right target. With the beacon, model reflected signal was adequately strong but the beacon antenna could be shielded from the ground station by the large booster, and in addition was subject to breakage. White Sands (Ref. 12) recommended a radar to firing site distance of some three miles, to ensure lock-on at fire.

Tracking of the model by kine theodolites had been poor, and it had been recommended during a meeting between Avro and C.A.R.D.E. personnel at Picton (Ref. 65) that certain modifications should be made to the kine's and accessories and that investigatory tests be carried out to improve contrast of model image on the film. Larger binoculars were tried and a better developing process was adopted. Tests were made with various filters using black and white film and a yellow "dayglow" model. Colour film was also used. Better correlation between kine time base and telemetery and tracking radar time base was also provided.

Concerning telemetery, a five point calibration on each subcarrier channel prior to and immediately after flight was to be made on all future tests, and the voice "count down" to be recorded on a separate channel. This "count down" had been one of the main causes of trouble that Bell had experienced in reducing model 5 data, the voice recordings overiding the "speedlock" or reference frequency.

During 1956, several T.T.V.'s were fired to provide tracking practice for kine operators.

On January 31st and February 1st T.T.V.'swere fired using a smoke trail. Tracking was poor and developing poor.

February 16th, tracking was much better. There was poor film definition, over exposure, dirty camera register and often no print of scale reading.

March 21st: for this T.T.V. test the doppler Velocimeter Radar was now functioning. However the Doppler tracked for only 2 secs. and kine tracking results were fair.

April 30th: this was a T.T.V. simulating separation as for the C-105 model, though the speed was too slow to be truly representative of the C-105 model. Kine tracking was good, doppler gave data from 2 secs. to 14 secs., while tracking radar was fair. The beacon antenna polarisation hampered radar tracking, and in addition the boresight film was poor.

June 6th: A T.T.V. with separation and a more representative speed. Fair to good tracking by 2 or 3 kines up to 15 secs., though the scale readings were often not clear and there was evidence of a dirty camera register. Doppler gave velocity data from 2 secs. to 15 secs., and tracking radar locked on with poor and intermittent boresight film, from 8 secs. to "splash".

The tests of April 30th and June 6th (Refs. 42 and 43) showed a considerable improvement in the measurement of model trajectory and speed. C.A.R.D.E. modified their claim for tracking radar performance, estimating it would begin at 10 secs., and it appeared that at least two kines would track it up to 10 secs., ensuring a trajectory record. Velocity from kine theodolites and tracking radar would be used only as a check of the velocity from doppler velocimeter radar. These velocities have been compared in Ref. 42. & Fig. 6

The Remaining Drag Models.

Free Flight Model #6 (Fig. 42)

With the same booster system, a drag model was made incorporating the latest aerodynamic modifications, such as 5% notch, 10% extensions, leading edge "droop", 30° conical radome and area rule over the armament bay.

Model 6 was fired at the N.A.C.A. station, Wallops Island, Virginia U.S.A. on May 9th 1956.

Telemetered data was recorded as before. The line of fire being out to sea, there were no kine theodolites. Trajectory data was obtained from an S.C.R. 584 modified) type radar which skin tracked the model continuously from 1 sec. after launch, on automatic mode except for the period of separation, when an experienced operator who was monitoring the oscilliscope display controlled the radar manually. Tracking corrections, normally supplied by two boresight cameras, one of 40" focal length and one of 80", were not available, from any early stage in the flight.

Velocity was obtained from doppler radar, corrected for trajectory and wind velocity, from .9 secs. to 20 secs.

Instrumentation was as follows:

Separation signal
Boost accelerometer
Drag "
Normal "
Transverse "
Angle of attack α
Angle of sideslip β
Pitot pressure
Static pressure (from probe on $\alpha - \beta$ vane)
Base pressure
Roll rate
Static buzz
Full rake pressure
Instrument bay temp.
Commutated duct pressures

On this model the $\alpha - \beta$ vane mounted on the sting was modified to include a probe to measure the static pressure. The assembly was balanced to within .1 ins. ozs. However, trouble was experienced in recording α, although β seemed good. While transverse acceleration and β correlated fairly well, normal acceleration and α showed marked disagreement.

Later tests showed that the α trace error was entirely due to the modifications to the $\alpha - \beta$ vane, but this was not immediately apparent. In the meanwhile it was assumed that the static probe would be fitted to the prototype aircraft, and the position error was determined over the complete test Mach range (See Fig. 25)

Because of the erroneous $\alpha - \beta$ vane and the unstable oscillations the test results were unsuitable for stability analysis but adequate for drag calculations. Drag was determined as for model #5 with similar corrections.

Observed in this test was the very high rate of roll associated with the unstable oscillations in the yaw plane. The derivative C_{n_β} was estimated (Fig. 26) and is discussed later.

Although velocity from doppler radar was used for test analysis, it was compared with velocity from integrated longitudinal accelerations, from pitot and probe static pressures and from pitot and radiosonde static pressures. (See Fig. 13)

On the pre-firing ground check, one commutated duct pressure was found inoperative, but in any event was duplicated. During boost the cover plate for the booster igniter came adrift, but caused no other damage and did not affect tracking radar.

(g) Free Flight Model #7

Fired at Wallops Island, Virginia, May 15th 1956. (Ref. 51) (Figs. 43, 44, 45)

This embodied all the aerodynamic modifications of model #6, with in addition more complete area rule affection the forward upper part of the fuselage.

Instrumentation was as in model #6. Base pressure did not function, and static "buzz" pressure gave a poor trace. Roll rate was even more violent, being approximately ± 300 degrees per second about a mean steady roll, at separation.

As on model 6, the static pressure from the $\alpha - \beta$ vane probe was calibrated with static press from radiosonde balloon over a range of Mach No.

Model velocity from the four sources were compared as on model 6. (Fig. 14)

With the principal axis tilted down at $\eta = 3^\circ 3'$ model 7 was affected by inertia coupling, as were models 5 and 6, so that a divergent oscillation was again obtained. The $\alpha - \beta$ vane malfunctioned in α in a manner similar to the model 6 test. Due to the inertia coupling effects these results were unsuitable for much stability analysis but were adequate for drag analysis which was performed as on model 5 (Fig. 24)

Tracking radar performance was better than that on model 6, the boresight cameras providing tracking corrections for all the useful part of the flight. Doppler performance was similar to that on model 6; however in the course of the radiosonde balloon ascent, a sharp wind reversal was noted, ("Eckmann Spiral"), (See Fig. 3) which would indicate that wind in that region was probably changing with time, causing model velocity to be less accurate in the region of 3000 feet altitude.

Results.

Booster motors performed within the limits expected, compared for boosters of models 1 and 2 in Fig. 1. Typical model trajectory and meteorological conditions of test are given in Figs. 2 and 3, while typical traces of telemetered data are reproduced in Figs. 4 and 5 covering a Mach No. range of approximately $1.7 > M > 1.15$. The presence of "inertia coupling" is apparent from Fig. 4, from the shape of the normal acceleration and sideslip traces. Angle of attack data was not good on models 6 and 7 due to the addition of a small thin probe on the front of the $\alpha - \beta$ vane body, to measure static pressure. On later modele this was rectified. However, the sideslip trace remained good, and the probe gave a fairly accurate record of the pressure as can be eeen from the calibration curve on Fig. 25. Some idea of the overall accuracy of telemetered data can be gained from the repeatability of these probe static curves, although there are several other factors contributing to the scatter; measurement of speed, measurement of radiosonde static pressure which ie the parameter, time variation of pressure between the two types of measurement, and dissimilarity of the probes. It is estimated that overall telemetering accuracy after reduction is within 1% of instrument full scale reading.

With the exception of model #3, which was not reduced, the model Mach numbers for the first seven models are given on Figs. 7 to 12, dynamic pressure, ($\frac{1}{2}\rho V^2$), on Fige. 15 to 20. Maximum Mach number attained ie approximately 1.7. Separation occupiee a very short but finite interval of time just after peak M is reached, after which the model instruments give a true picture of air forces on the model. Values of M and q for models 1 and 2 have only a limited accuracy; as kine-theodolites failed to track the model and estimated trajectory was used.

Where model velocity from Doppler Velocimeter Radar was available, the model Mach numbers obtained from four different sources have been compared. Mach No. could be computed from:

(i) Doppler Radar, allowing for model trajectory, air velocity and temperature

(ii) Kine theodolite readings, allowing for air velocity and temperature

(iii) Integrated drag acceleration, allowing for air velocity and temperature and altitude.

(iv) The ratio of pitot pressure to probe static pressure

(v) The ratio of pitot pressure to radiosonde static pressure

(vi) In an approximate form, from tracking radar, allowing for air velocity and temperature. Here the model space distance travelled must be measured over a large interval of time, say 2 secs., to give reasonable accuracy.

For models 6 and 7, Mach No. from sources (i) (iii) (iv) and (v) have been compared on Figs. 13 and 14.

To indicate the order of accuracy of speed measurement by kine theodolites, model space velocity for a Test Tracking Vehicle (D.T.T.V. #2) has been compared on Fig. 6 with that from doppler radar.

On models 4 and 5, kine theodolites were used to determine model speed, in conjunction with integrated accelerometer readings, while on models 1 and 2 only accelerometer readings were available to compute speed. For models 6 and 7, model speed was based on doppler radar.

The accelerometers, being located very near to the model centre of gravity, gave true measurements of the air loads on the model. Then drag,

$$D = A \cos \alpha - Z \sin \alpha \text{ and } C_D = \frac{D}{qS}$$

This total model drag is plotted on Figs. 22, 23, 24 for models 5, 6, and 7, along with the drag corrected to apply to full scale C-105 airframe, computed by Avro Aerodynamic Performance Section. (See Appendix "A"). Drag of models 1 and 2, shown on Fig. 21 is of limited accuracy because of the uncertainty of speed and the absence of an angle of attack measurement.

The ratios of model and full scale radii of gyration compared in Table I are practically the same in all three planes.

The period of oscillation is approximately proportional to $\sqrt{\mu}$ and k.

or: $\frac{\text{Period of Model}}{\text{Period of C-105 at same V and h}} = \sqrt{\frac{\mu_m}{\mu_A}} \cdot \frac{k_m}{k_A}$

∴ Ratio of periods in roll = .29
Ratio of periods in pitch = .31
Ratio of periods in yaw = .30

The three ratios are very similar, thus providing a good measure of dynamic similarity.

A simple method of determining preliminary values of the derivatives C_{n_β} and C_{M_α} from test results is to assume single degree of freedom motion. Then:

$$C_{n_\beta} = \frac{4\pi^2}{P^2} \cdot \frac{I_z}{57.3qSb} \qquad (1)$$

$$C_{M_\alpha} = \frac{-I_y}{57.3qS\bar{c}} \left[\frac{4\pi^2}{P^2} + \frac{.480}{(T_{\frac{1}{2}})^2} \right] \qquad (2)$$

Although it was not intended to determine Stability data from the first seven models, it is interesting to compare the approximate value of C_{n_β} from models 4, 5, 6 and 7 with that obtained by a rigorous method from later yaw stability models 8 and 9. (For complete analysis of models 8 and 9 see Refs. 72&73)

Because of the slab wing section, crude models 1 to 4 were not suitable for approximate analysis of C_{M_α}; nor were models 5, 6, and 7, due to the "inertia coupling" which caused divergent oscillations for part of the flight.

From Fig. 26A, which gives variation of the mean Reynolds Number during the tests, it may be seen that at M = 1.60 the model R = 44 x 10^6, is equivalent to

CONFIDENTIAL

that of the full scale C-105 at approximately 56,000'. By comparison, the mean R at M = 1.6 during the Wind Tunnel tests at Langley was 2.68×10^6. This illustrates the realistic order of Reynolds number the free flight tests can provide.

The "inertia coupling" referred to in the motions of models 5, 6, and 7 was caused by the principal axis being depressed on the models. ($\eta = 3^{\circ} 23.8'$ mean), more than on the C-105 ($\eta = 1^{\circ} 42.5'$) mainly due to the oversize fin on the models. This coupling is present as one of the destabilising terms in the equations of motion, such that any rolling acceleration produces a yawing acceleration. This yawing acceleration would produce sideslip which in turn would cause a rolling acceleration. Under certain circumstances, that is with principal axis depressed sufficiently, the model motion could become divergent, which is what happened on models 5, 6, and 7.

Analog computer studies were made, (71) with five degrees of freedom using typical model weight, inertias, geometry, flight conditions, and estimated aerodynamic properties. It was found that although stable motion was produced from these inputs, slight variation of the aerodynamic derivatives, within the likely accuracy of estimation, caused divergent motion similar to that obtained during the free flight model tests. Reduction of the principal axis angle to $1\frac{1}{2}^{\circ}$ again produced stable motion on the analog. Subsequent models 8, 9, 10 and 11 were therefore ballasted and equipment re-located to give a value of η close to $1\frac{1}{2}^{\circ}$, or approximately C-105 value, with the result that the motions of these models were well damped.

1319 A

Conclusions, and Suggestions for Future Free Flight Work.

In all, the tests were remarkably successful. The first two "Crude" models evaluated the test system as a whole, and while on the third "crude" model the yaw impulse mechanism failed to operate, this malfunction was remedied on the fourth model, on which a large amount of telemetery was tested.

The three "Drag" models provided all the data required to evaluate supersonic airframe drag, and in addition served as a preliminary and mainly qualitative assessment of the C-105 dynamic stability.

Drag was slightly higher than previously estimated. The benefit from the two types of "Area Rule" modifications to the fuselage contours, along with other slight configuration changes may be seen between Fig. 22 and Figs. 23, 24.

The first seven firings were achieved with 100% successful launch, boost, separation and model free flight, a record which compares very favourably with that of any other free flight programme.

From the subsequent test of models 8 and 9 it was found that the disturbances in pitch and yaw from the divergent motion of models 6 caused only slight increase in drag. However, in future free flight tests the effect on drag of such motion may be more pronounced, making it all the more important to eliminate such instability, using tools such as the analog computer or the ballistic range.

The present series of drag model tests provided the supersonic model drag with reasonable accuracy, which was the requirement. To obtain good transonic and subsonic drag it is essential to have a pitot-static pick up in a position of undisturbed flow on the model, for as model speed decreases the percentage of the true air speed which the rather uncertain wind velocity represents, increases, and one has to rely on pitot-static tube for true model airspeed. There should also be an additional longitudinal accelerometer and an additonal pitot pressure transducer, to cover the low values of pitot pressure and drag acceleration at the low airspeeds. More complete recommendations will be made in Reference 72

APPENDIX 'A'

Drag corrections applied to the Dreg Free Flight Model results to make them more representative of CF-105

Details of calculations involved may be found in Ref. 70.

1. Base drag correction is required because the edges of model duct exit were made more blunt than C-105, to transmit the loads during boost.

2. Momentum drag correction is required since Avro cherges momentum drag egainst engine thrust.

3. Induced drag correction.

4. Allowance is made for the difference between model and aircraft exit flow from the nozzle (Ref. 69 used)

5. Spillage drag correction is required since Avro cherges Spillege drag egeinst engine thrust.

6. On the model there was an additional and out of scale ventral pitot tube.

7. The models contained an out of scale pressure rake located in the duct exit. (Refs 67, 68, used).

8. The fixed elevator setting of the models requires a trim drag correction.

9. Model fin is larger than C-105. (See Figs. 30 to32)

10. Correction for α - β vane installation

11. Fuselage contour differences, where applicable.

Instantaneous Drag Values

Due to the oscillatory nature of conditions during the flight of the free flight rocket models, the resulting test data shows a certain scatter in values. In processing this data scatter is eliminated by drawing a mean curve through a series of test points.

At M = 1.5 the instantaneous data was used to determine an instantaneous drag coefficient. Since this data did not lie exactly on the averaged curves a slight difference results between instantaneous corrected $C_{D_{MIN}}$ and the average value at M = 1.5, as shown on Figs. 22 to 24

A typical instantaneous drag value, on F.F.M. #5 at M = 1.5, is listed in Table II.

REFERENCES

1	P/F.F.M./1	Firing of F.F.M. 1 & 2 (January 55)
2	P/F.F.M./4	Data reduction techniques (June 55)
3	P/F.F.M./5	Time lags of pressure systems (February 55)
4	P/F.F.M./6	Yaw disturbance calculations. (February 55)
5	P/F.F.M./7	PAL 1-2 Accelerometer (March 55)
6	P/F.F.M./11	Operating characteristics of PAL 1-2 accelerometer. (July 55)
7	P/F.F.M./12	Firing of F.F.M. 3, 5 & 4 (July 55)
8	P/F.F.M./13	Battery activation. Visit to Eagle Picher (July 55)
9	P/F.F.M./14	Data reduction of F.F.M. 5 (July 55)
10	P/F.F.M./15	Static probe modification to α - β vane (September 55)
11	P/F.F.M./16	Repeatability and temperature tests on various types of pressure transducers (October 55)
12	P/F.F.M./17	Visit to White Sands proving grounds and Resdel Engineering Co. with respect to Doppler Radar (November 55)
13	P/F.F.M./18	The α - β vane (November 55)
14	P/F.F.M./19	Doppler radar, recording and data reduction (December 55)
15	P/F.F.M./20	Moment of Inertia test procedures. (January 56)
16	P/Models/7	C-105 free flight model (January 53)

34	P/F.F.M./8	Flight data, F.F.M. 3 (June 55)
35	P/F.F.M./9	" " F.F.M. 4 (June 55)
36	P/F.F.M./10	Flight data, 1st drag model F.F.M. 5 (June 55)
37	P/F.F.M./22	Rawinsonde, tracking and doppler F.F.M. 6 (June 56)
38	P/F.F.M./24	Rawinsonde, tracking and doppler F.F.M. 7 (June 56)
39	P/F.F.M./23	Reduced telemetery data F.F.M. 6 (June 56)
40	P/F.F.M./25	Reduced telemetery data F.F.M. 7 (June 56)
41	P/F.F.M./26	Data from kine theodolites F.F.M. 4 & 5 (August 55)
42	P/F.F.M./27	D.T.V. #1 & D.T.V. #2 fired at Picton. Data reduction (July 56)
43	P/F.F.M./28	Evaluation of range with D.T.V. #1 & D.T.V. #2 (July 56)
44	P/F.F.M./31	Flight data and data reduction F.F.M. 6 (November 56)
45	P/F.F.M./32	Flight data and data reduction F.F.M. 7 (November 56)
46	P/F.F.M./33	Flight data and data reduction F.F.M. 8 (November 56)
47	P/F.F.M./34	Flight data and data reduction F.F.M. 9 (November 56)
48	P/F.F.M./35	Flight data and data reduction F.F.M. 10 (November 56)
49	P/F.F.M./36	Flight data and data reduction F.F.M. 11 (November 56)
50	P/F.F.M./37	Kine theodolite survey data and general kine data reduction (November 56)

CONFIDENTIAL
UNCLASSIFIED

AVRO AIRCRAFT LIMITED MALTON - ONTARIO TECHNICAL DEPARTMENT		REPORT NO. P/F.F.M./47	
		SHEET NO 32	
AIRCRAFT: C-105		PREPARED BY D. Ewart & W. Taylor	DATE July 1957
		CHECKED BY	DATE

51	P/F.F.M./21	Summary of firings of F.F.M.'s 6 & 7. (June 56)
52	P/Models/41	Free Flight Model moments of inertia. Preliminary report of theory, corrections and procedure. (December 54)
53	P/Models/42	Crude model moments of inertia based on swing tests (January 55)
54	P/Models/43	Tests to check and prove system and method used for swinging F.F.M.'s (January 55)
55	P/Models/49	Weights, C.G.s and moments of inertia for drag models. (March 55)
56	P/Models/50	Estimates of weights, C.G.s and moments of inertia of further F.F.M.'s (May 55)
57	P/Control/45	Longitudinal dynamic response of C-105 F.F.M. due to elevator deflection (July 53)
58	P/Stab/44	Lateral stability of model booster combination (March 54)
59	P/Stab/51	F.F.M. trajectory after separation, elevators checked at 2^o, launch at 45^o. (July 54)
60	P/Stab/63	Preliminary data reduction and comparison with theory F.F.M. 1 & 2 (January 53)
61	P/Stab/64	Lateral stability and trajectory, F.F.M. & "Terrier" booster (July 54)
62	P/Stab/113	Calculation of lateral derivatives and dynamic stability of F.F.M. 6 & comparison with tests. (June 56)
63	P/Stab/29	Determination of downwash and longitudinal stability, F.F.Models. (August 53)
64	P/Models/24	Investigation of longitudinal stability, F.F.Models. (March 54)

65 Minutes of Kine Theodolite meeting at C.A.R.D.E. Range, Picton, on June 14th 1955.

66 7-0400-44 issue 3. C-105 Mk I Weight summary and C.G. position (March 57)

67 R.Ae.S. Data Sheets - Aerodynamics

68 Aerodynamic Drag - Hoerner.

69 N.A.C.A. RM.E54.J.26

70 P/Aero Data/66 Drag of Free Flight Models.

71 P/Stab/128 Some dynamic stability studies of free flight models.

72 P/F.F.M./48 Summary of F.F.M. tests and results. (F.F.M.'s 8 to 11) (Estimated September 57)

73 P/F.F.M./57 Free flight stability model results. (July 57)

74 P/Stab/128 Some dynamic stability studies of C-105 F.F.M.'s (December 56)

75 P/Stab/132 Dynamic equations relative to body axes. (January 57)

76 P/Models/24 Longitudinal investigation of free flight models. (March 54)

TABLE I

Model Weights and Inertias

	Wt.	I_x	I_y	I_z	η	C.G.
F.F.M. #1	463	12.63	73.53	83.86	2° 50.19'	.25
#2	456	12.60	72.24	82.53	2° 45.43'	.25
#3	472	13.37	78.9	88.23	2° 27.15'	.25
#4	474	13.45	78.5	88.75	2° 15. 5'	.25
#5	465	11.72	70.1	79.37	3° 47.33'	.25
#6	482	11.79	73.25	81.30	3° 21.15'	.25
F.F.M. #7	484	11.90	72.02	79.97	3° 3'	.25

Mean values of F.F.M.'s 5, 6 and 7 at c.g. of 25% MAC

k_{x_m} = .895' W = 477 lb.

k_{y_m} = 2.204'

k_{z_m} = 2.330' W/S = 24.9

η = 3° 23.8'

Corresponding C-105 values, 55,000 lb. wt. (and 1,522 lb. ballast) at c.g. of 29.94% MAC.

1/8 k_{x_A} = .825' W = 55,000 lb.

1/8 k_{y_A} = 1.883'

1/8 k_{z_A} = 2.030' W/S = 44.9

η = 1° 42.5'

$8 \cdot k_{x_m}/k_{x_A}$ = 1.084

$8 \cdot k_{y_m}/k_{y_A}$ = 1.170

$8 \cdot k_{z_m}/k_{z_A}$ = 1.147

and Ratio of wing loading $\frac{(W/S)\text{model}}{(W/S)\text{C-105}}$ = .555

TABLE I (Continued)

Approx. Estimated Static Margin of Model and Booster (ins.)

	Longitudinal	Lateral
Subsonic	18	43
Supersonic	22	50

TABLE II

F.F.M. #5

Instantaneous Corrected Drag, M = 1.5

Measured C_D = .0278 at M = 1.5

Corrections

Momentum Loss	.00126
Base Drag	.00063
Pressure Rake (Exit)	.00006
Shock Losses (Exit)	.00050
Elevator Angle	.00150
Fuselage Contour Difference	.00085
Larger Fin	.00035
Spillage Drag	-.00021
Pitot Tube	.00024
α - Vane	.00020
Total C_D	.00538

$\therefore$ C_D corrected = .0224

UNCLASSIFIED

CONFIDENTIAL

P/FFM/47 FIGURE 1

D.E. Ewart. 18. I. 55

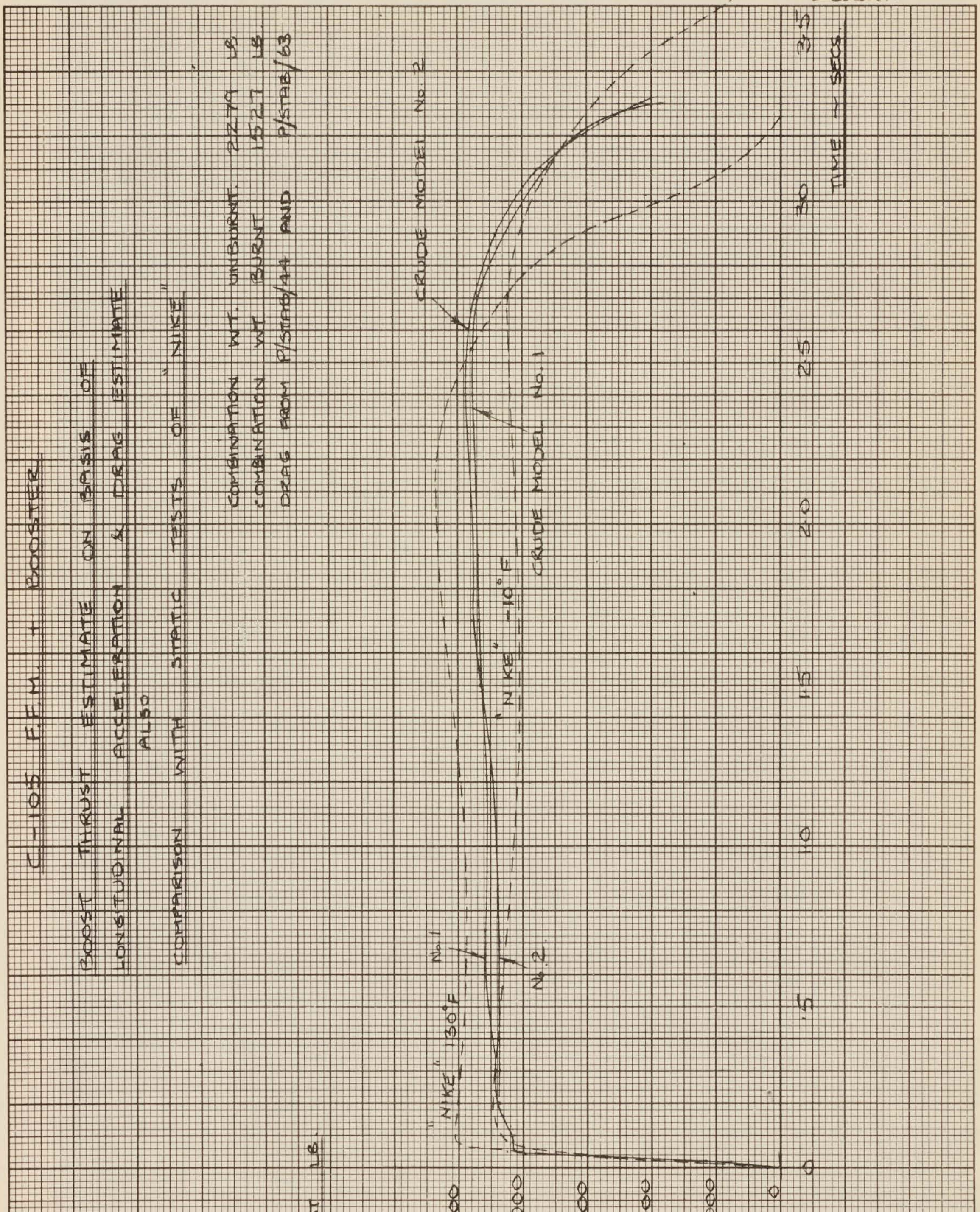

FIG. 3

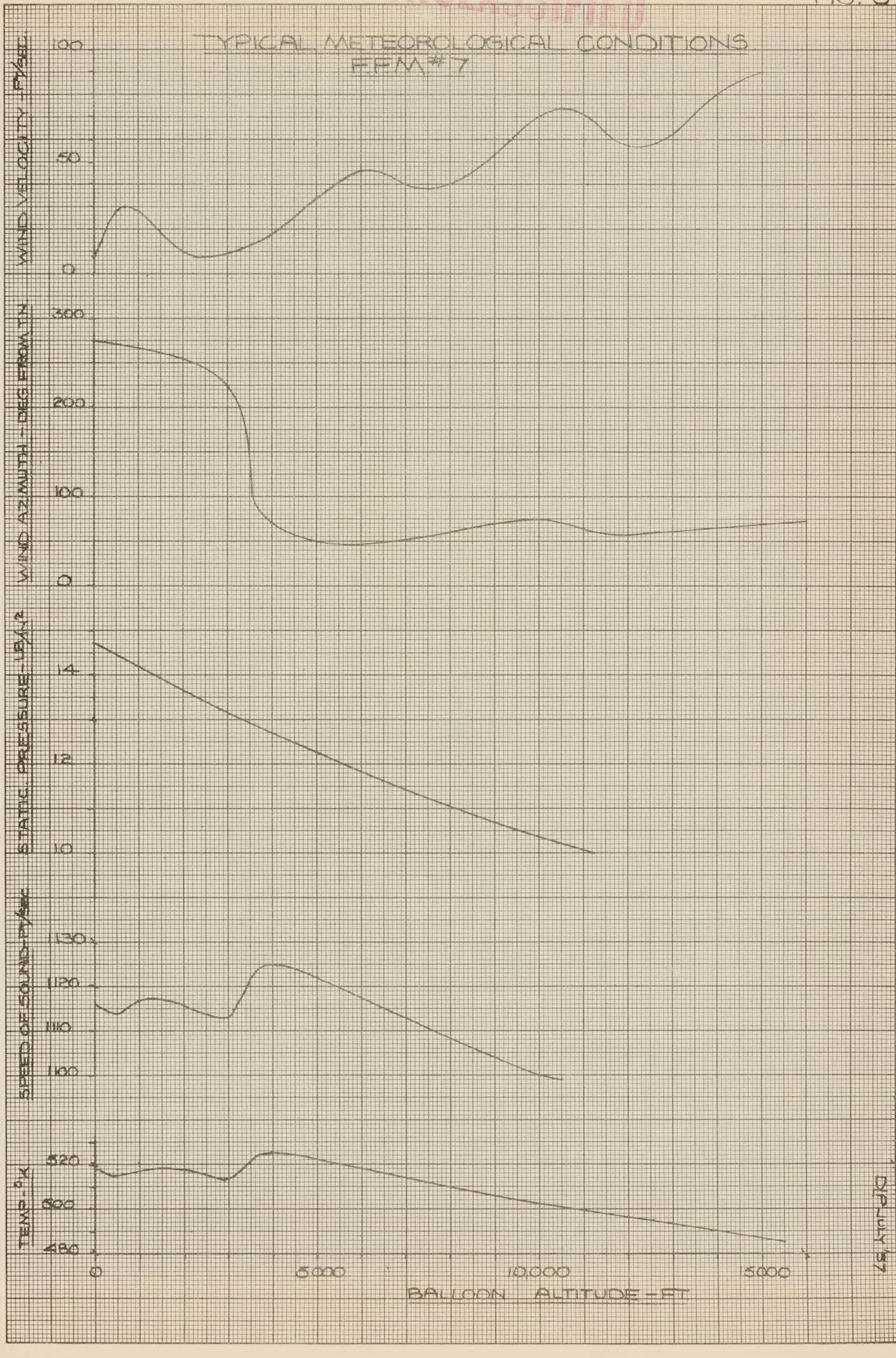

P/FFM/47 FIG. 3
DP JULY '57

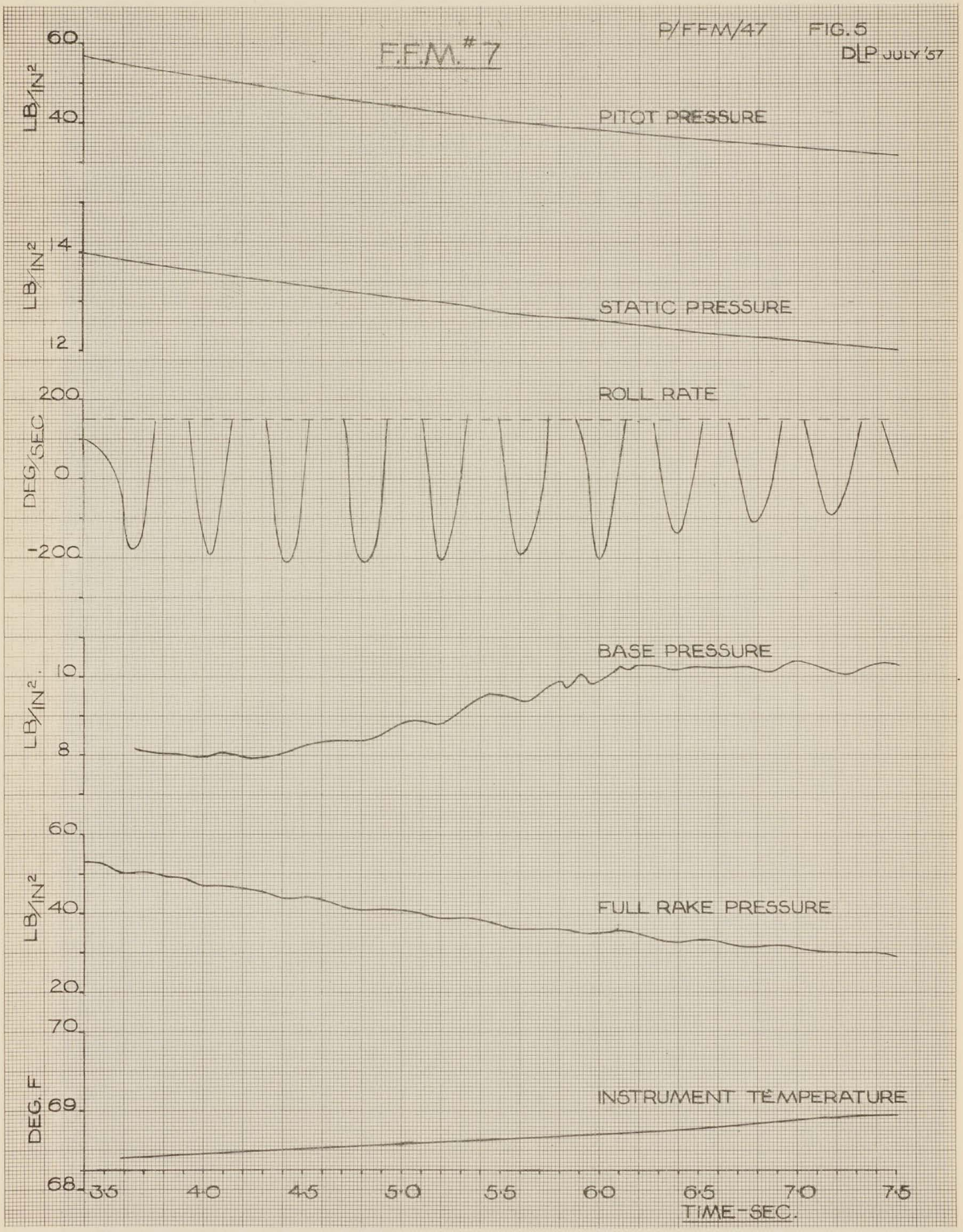
P/FFM/47
FIG. 5
D.L.P. JULY '57
F.F.M. # 7
LB/IN²
60
40
PITOT PRESSURE
LB/IN²
14
12
STATIC PRESSURE
200
ROLL RATE
DEG/SEC
0
-200
BASE PRESSURE
LB/IN².
10
8
60
LB/IN²
40
20
FULL RAKE PRESSURE
70
DEG. F
69
68
INSTRUMENT TEMPERATURE
3·5
4·0
4·5
5·0
5·5
6·0
6·5
7·0
7·5
TIME-SEC.

UNCLASSIFIED

FIG. 7

FIG. 7
P/FFM/47

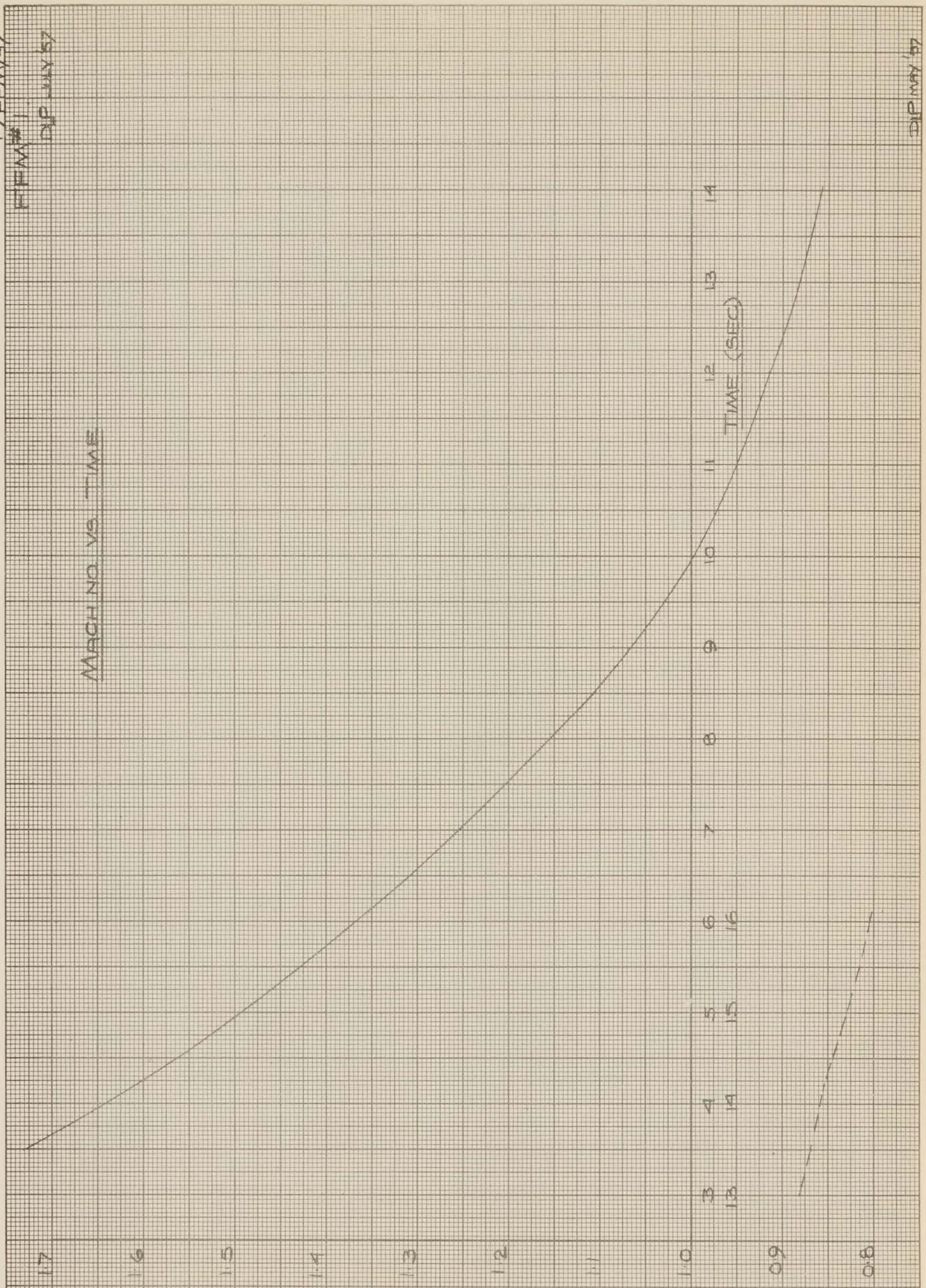

UNCLASSIFIED

FIG. 8

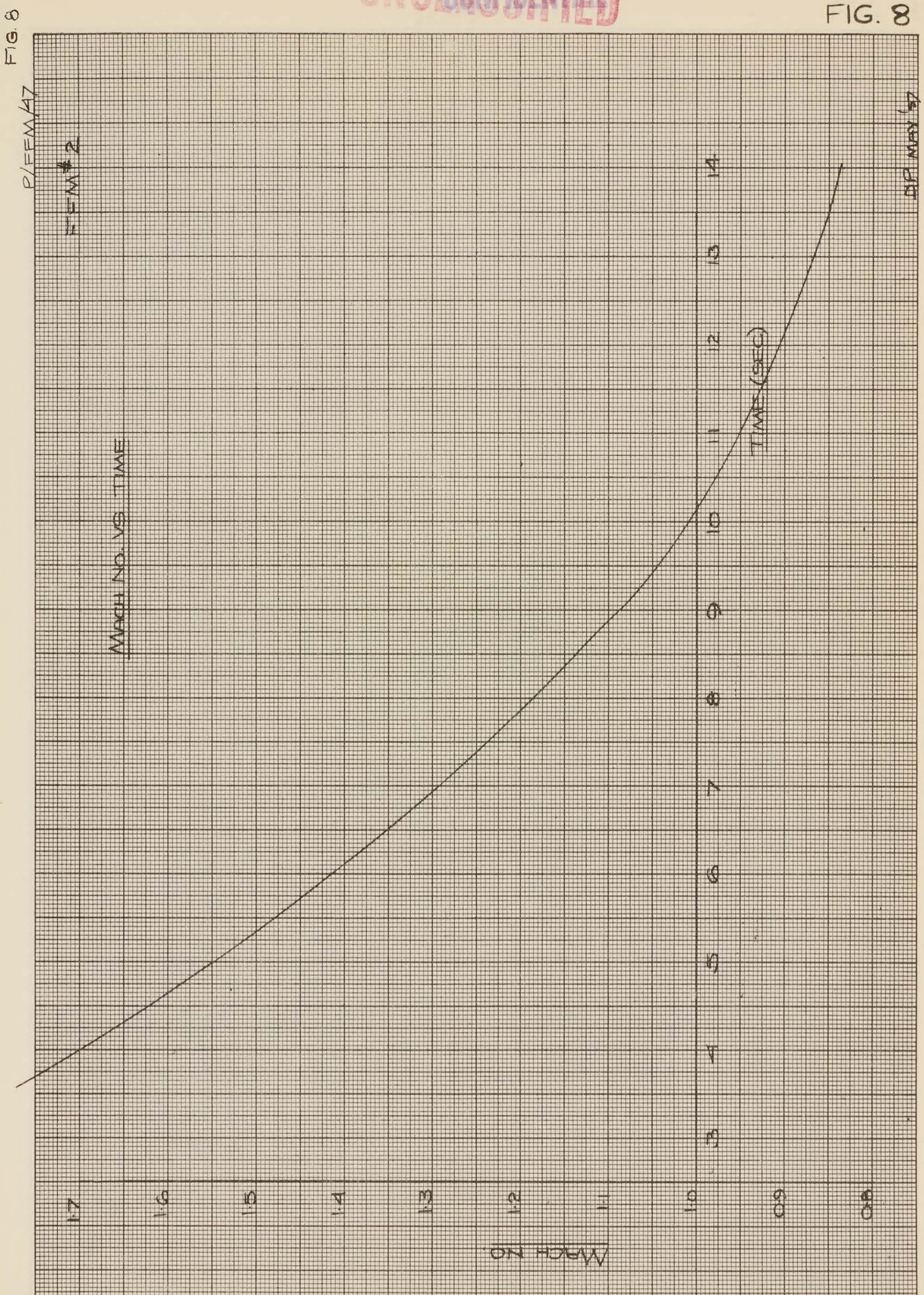

CONFIDENTIAL

UNCLASSIFIED

FIG. 9

FIG.9

P/FFW/47

DBC 20.7.55

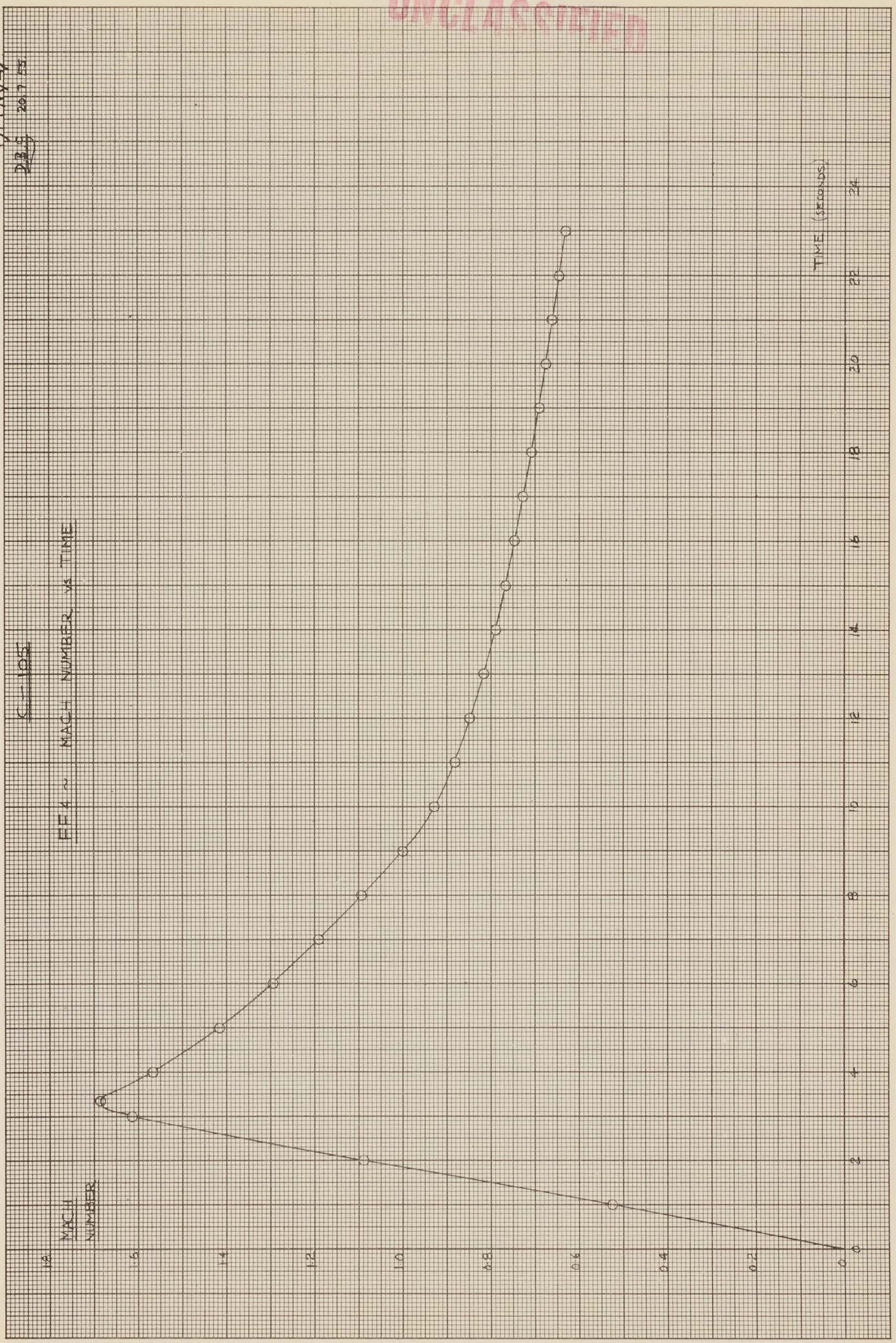

UNCLASSIFIED

FIG. 10

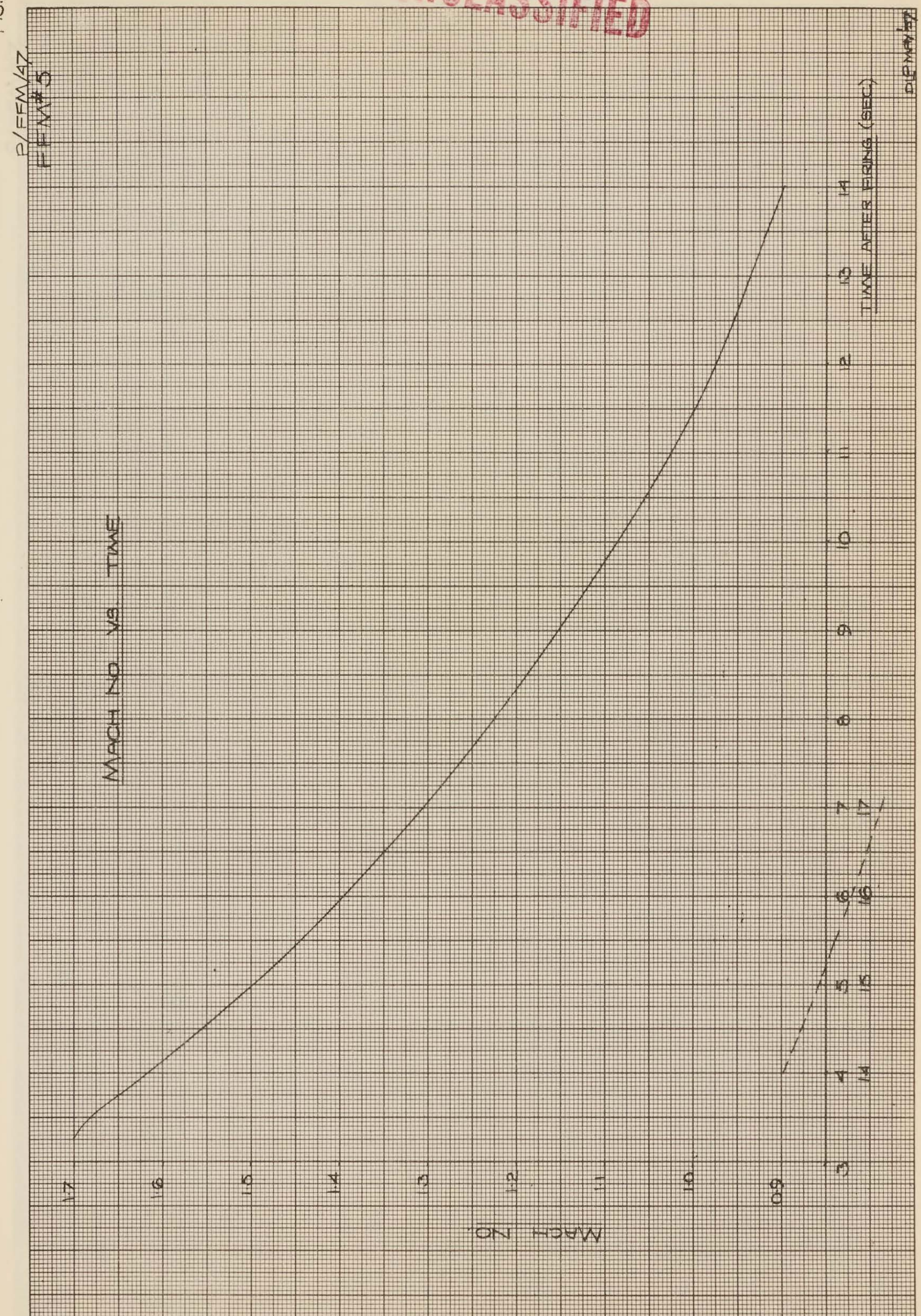

FIG.10

FIG. 12
P/FFM/47

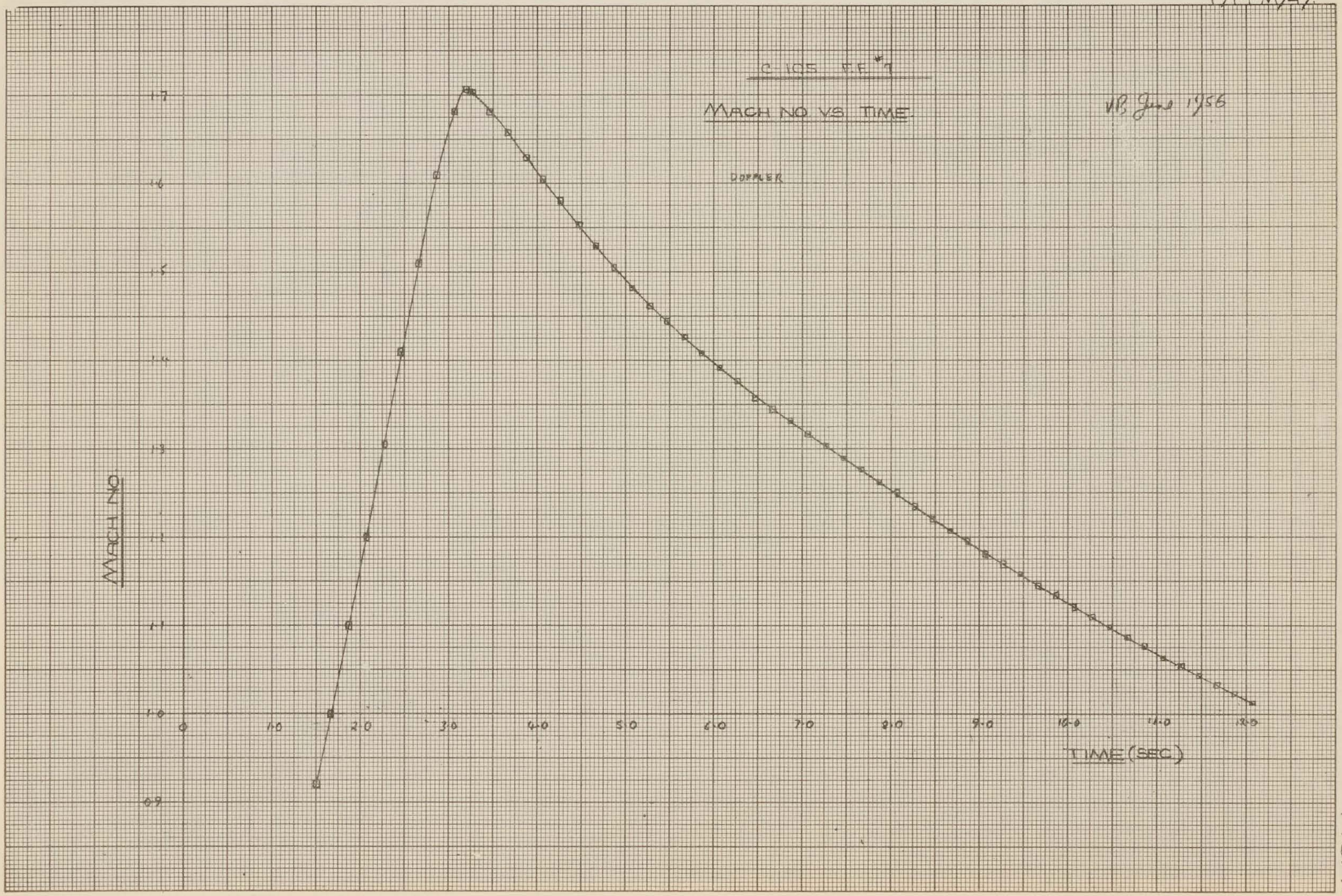

FIG. 12

P/FEM/47 FIG. 13.

CONFIDENTIAL

UNCLASSIFIED

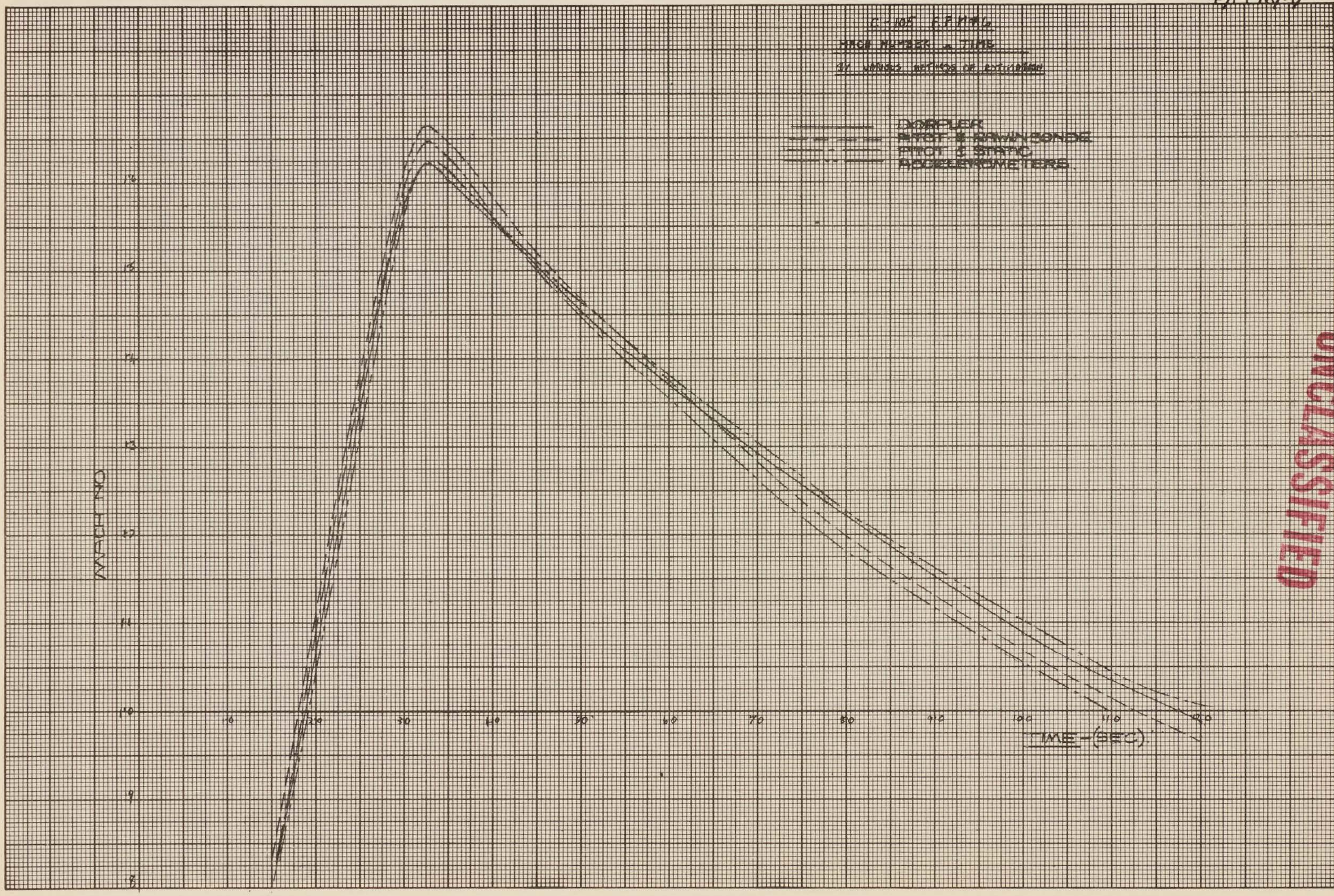

FIG. 13

FIG. 15

P/FFM/47

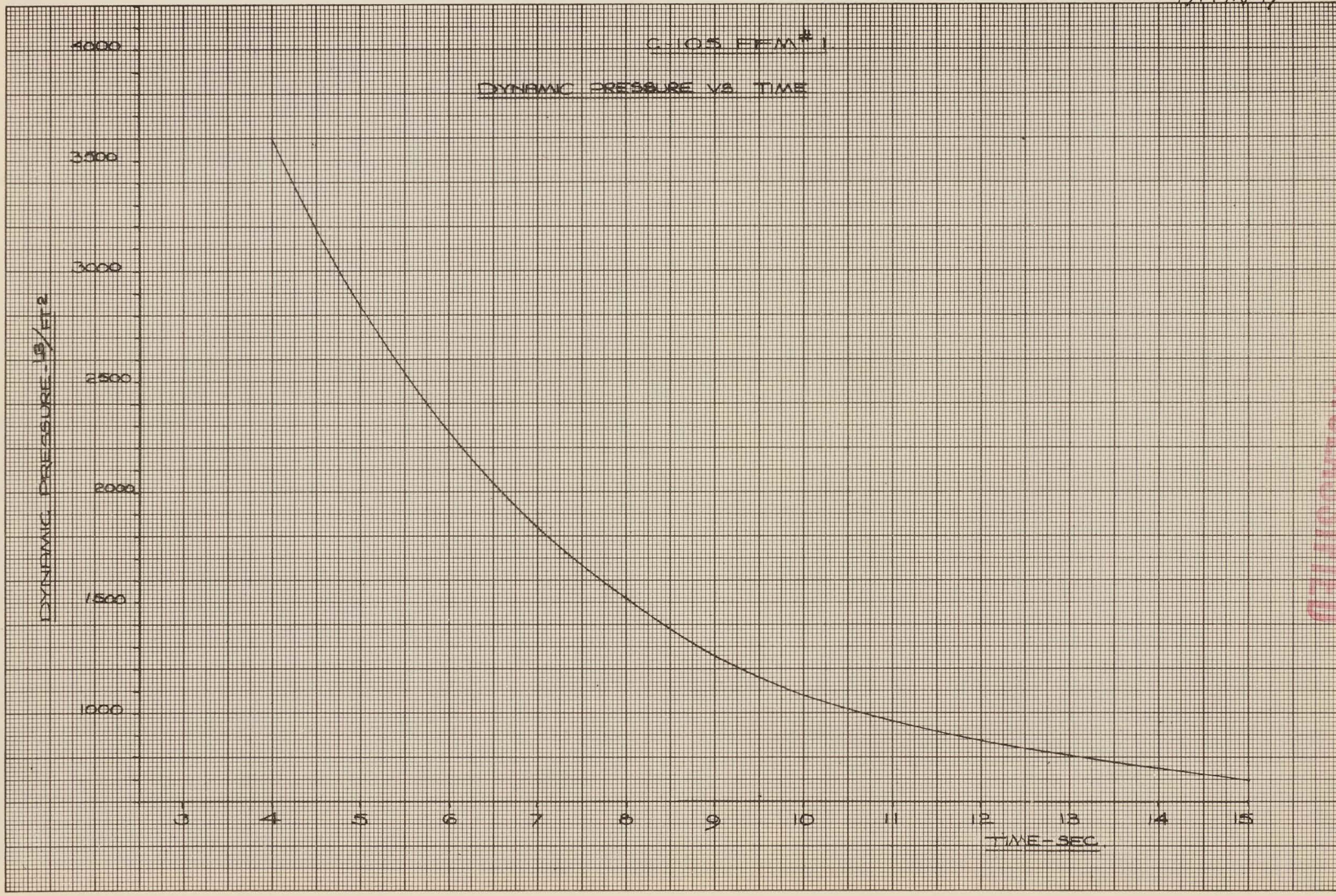

CONFIDENTIAL

UNCLASSIFIED

FIG. 15

FIG. 16

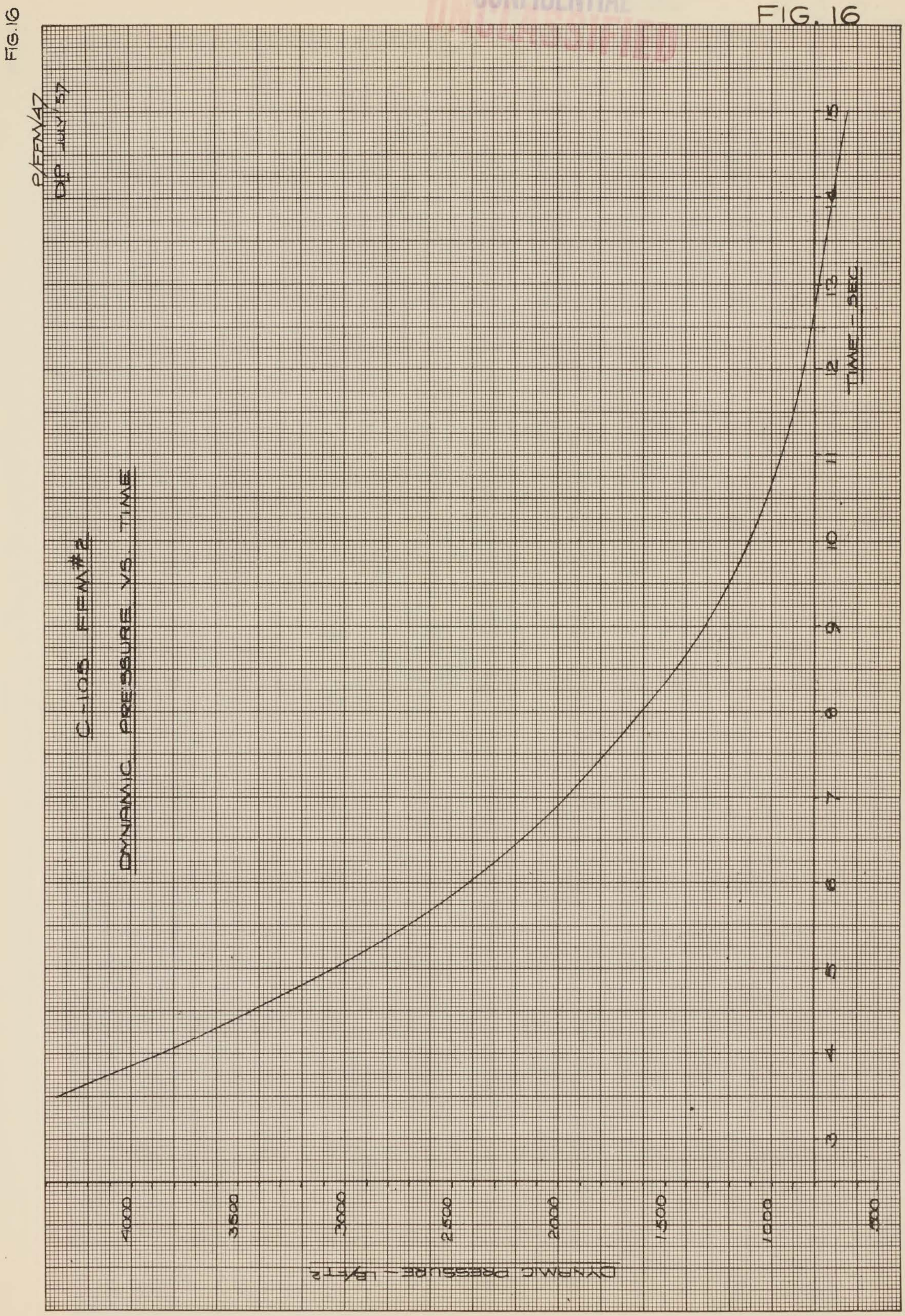
FIG. 16
P/FFM/47
DP JULY '57
C-105 FFM #2
DYNAMIC PRESSURE VS TIME
TIME - SEC
3
4
5
6
7
8
9
10
11
12
13
14
15
DYNAMIC PRESSURE - LB/FT²
4000
3500
3000
2500
2000
1500
1000
500

FIG. 19

P/FFM/47.

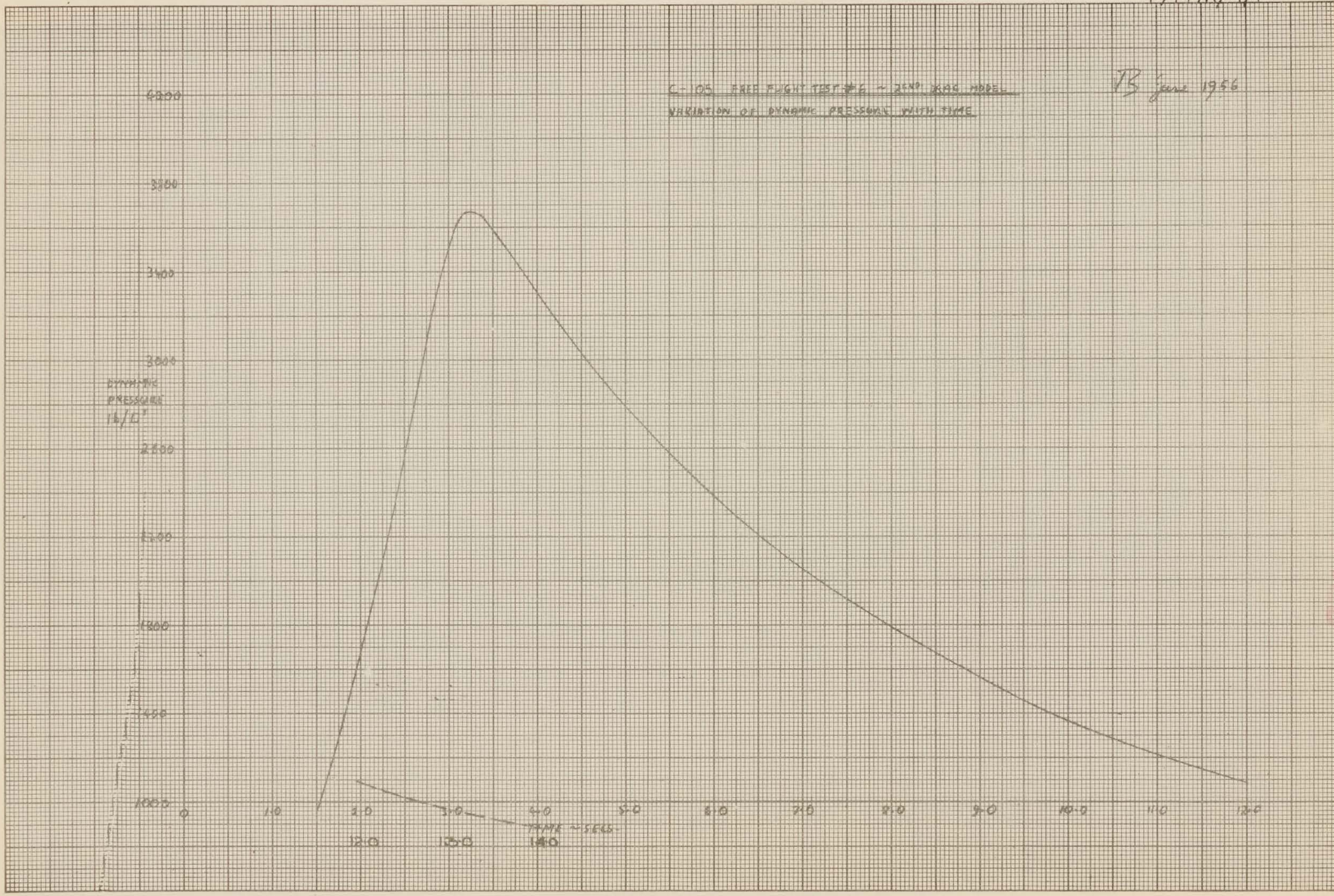

FIG. 19

FIG. 20.

P/FFM/47

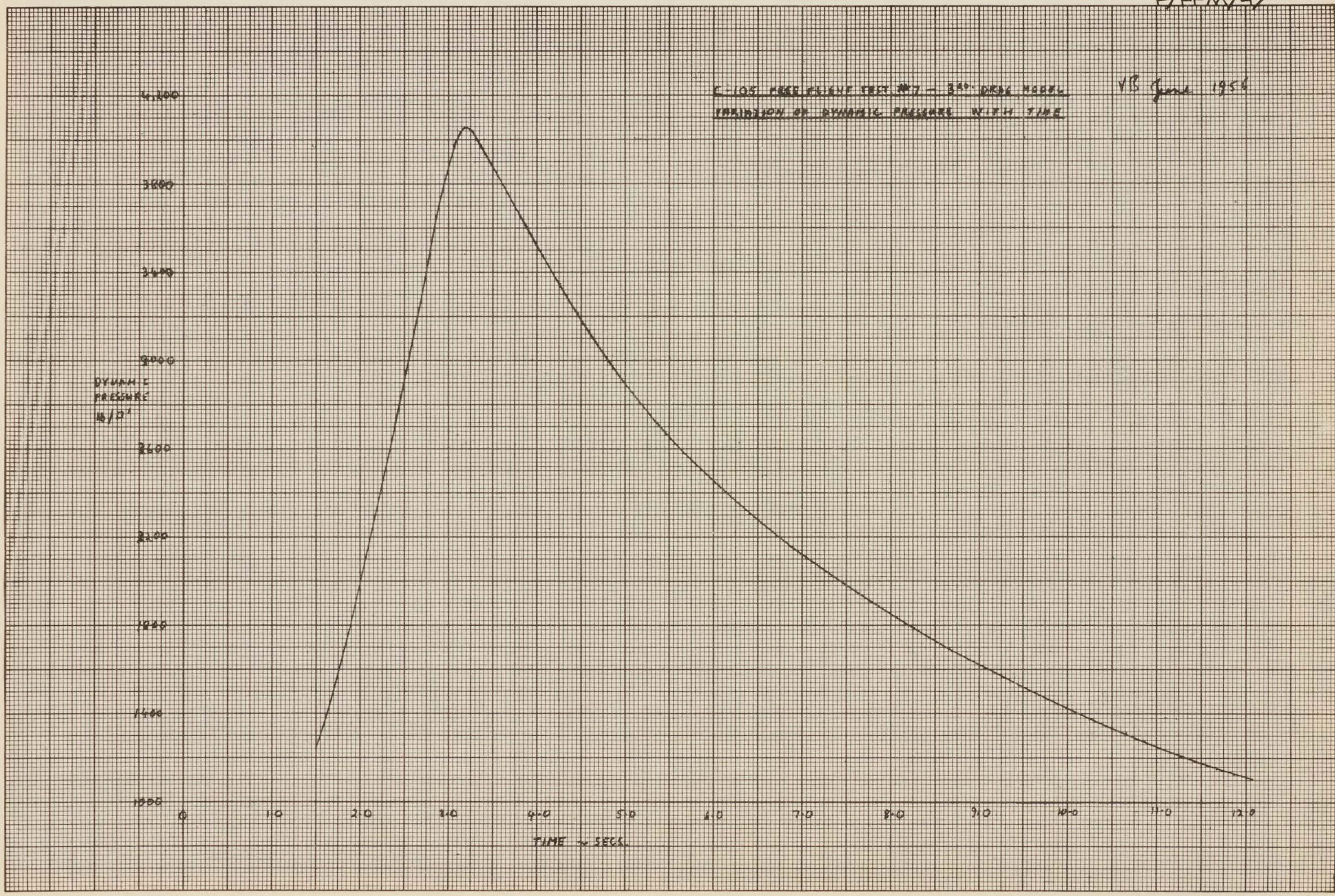

FIG. 20

FIGURE 22

P/FFM/47

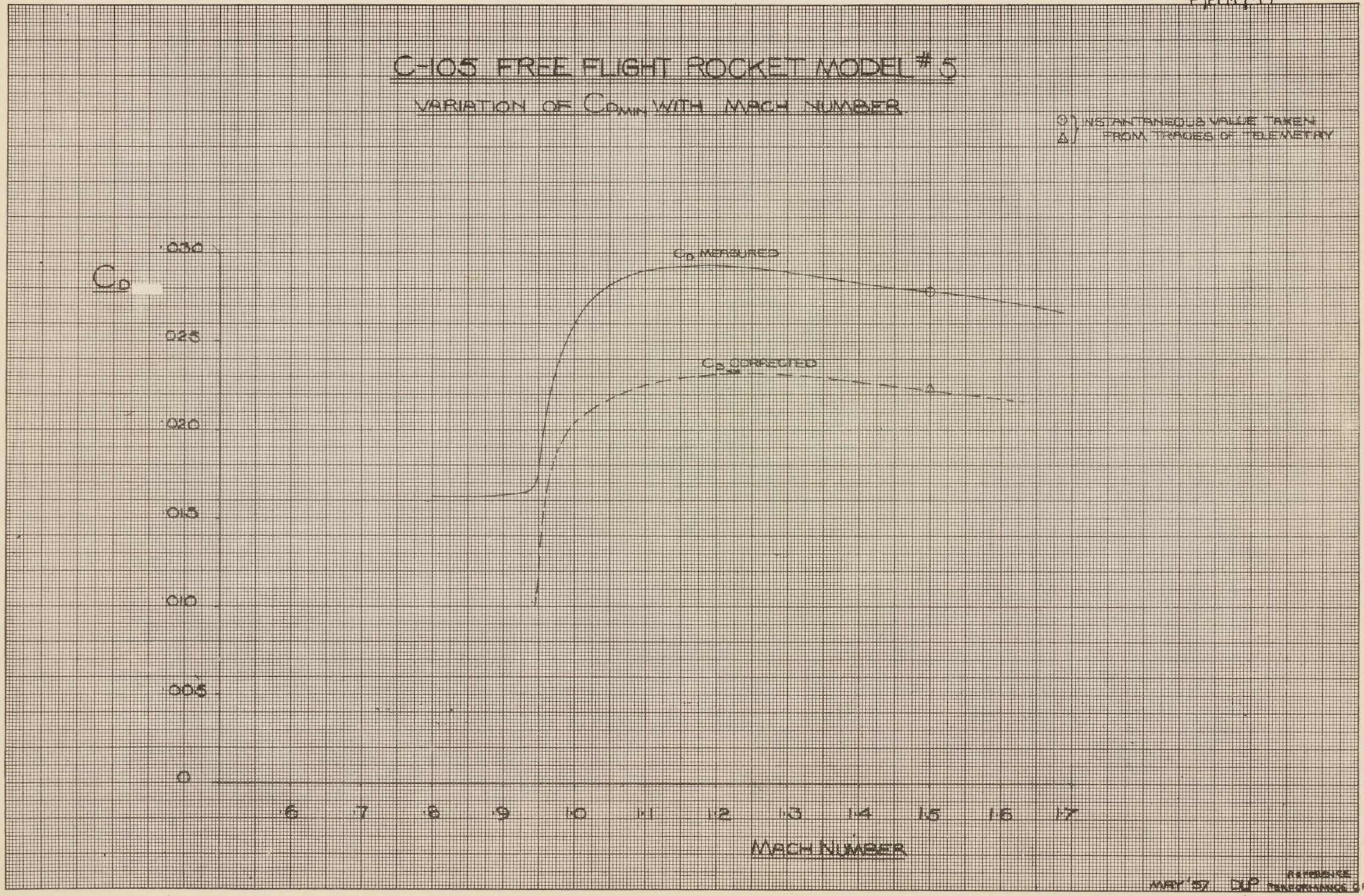

MAY '57 DLP PERFORMANCE GROUP

FIG. 22

FIGURE 23
P/F.F.M/47

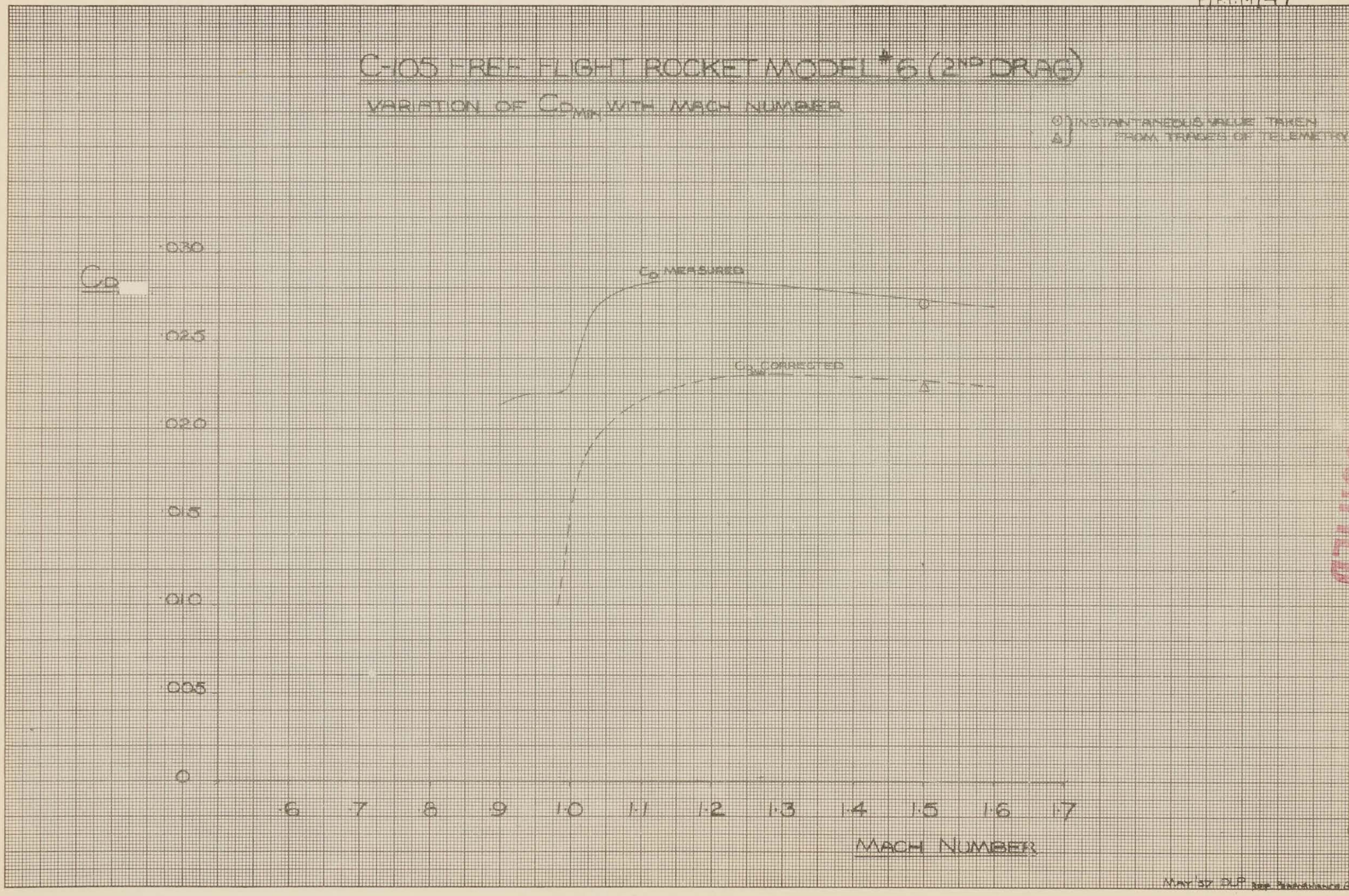

FIG. 23

P/FFM/47

FIG. 24

C-105 FREE FLIGHT ROCKET MODEL # 7 (3RD DRAG)

VARIATION OF $C_{D_{MIN}}$ WITH MACH NUMBER

○ } INSTANTANEOUS VALUE TAKEN
△ } FROM TRACES OF TELEMETRY

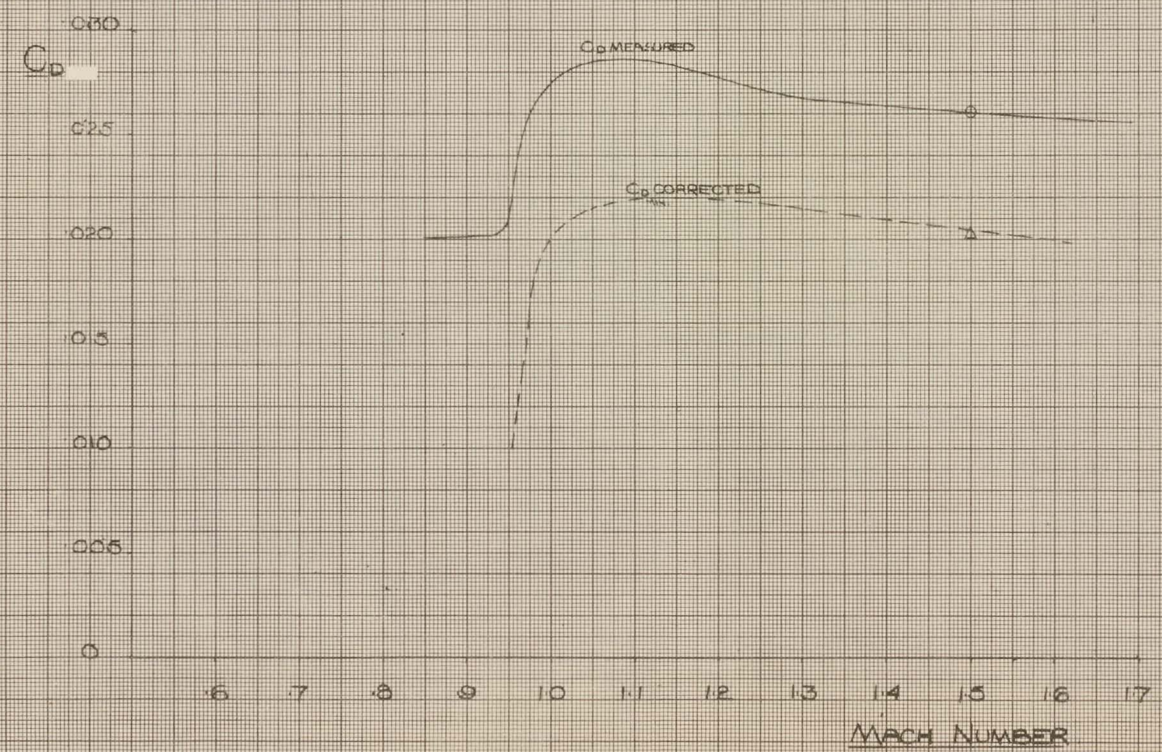

MAY '57 DLP Aero. Performance Group

C-105

CRUDE FREE FLIGHT MODELS

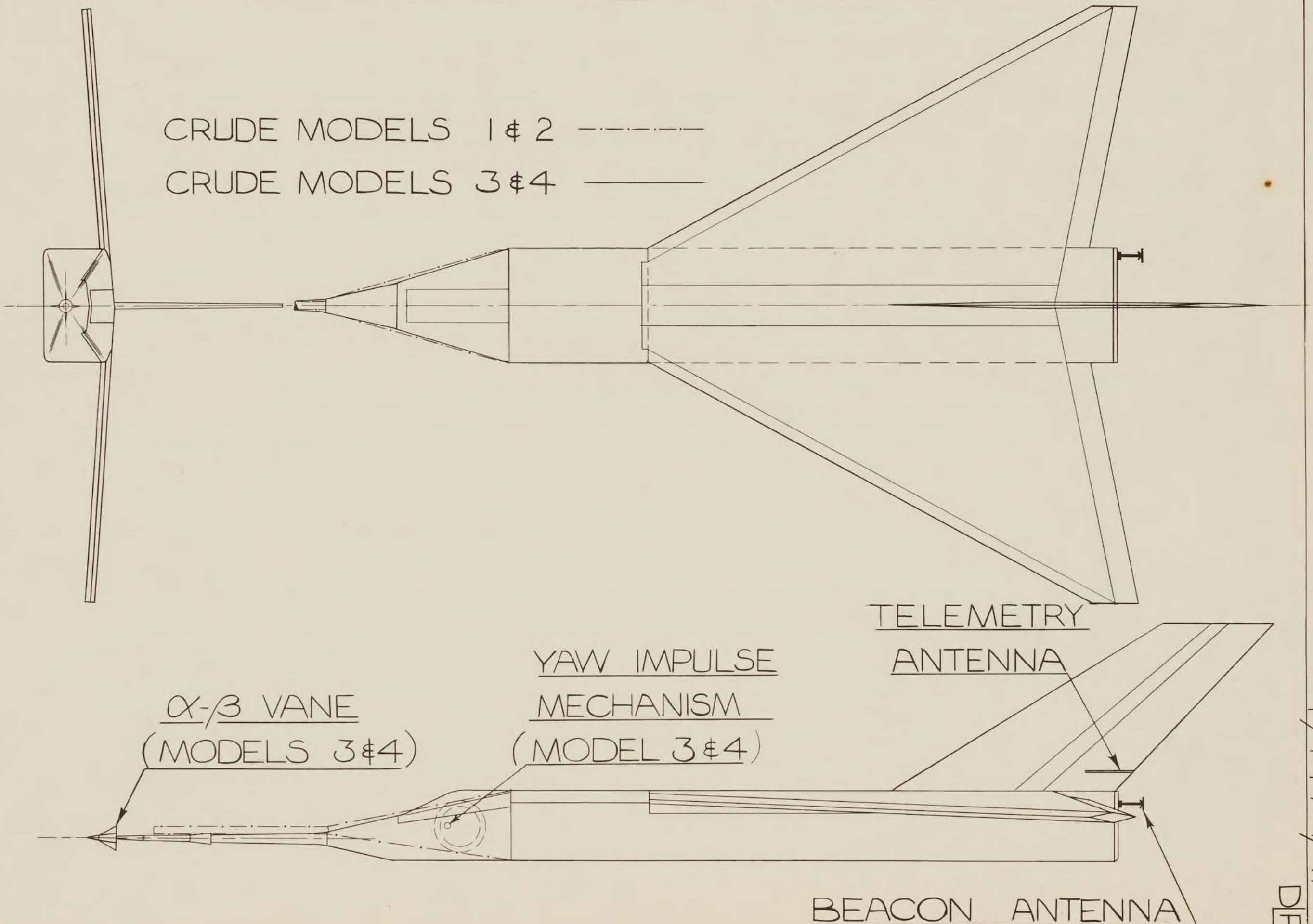

UNCLASSIFIED

P/FFM/47
FIG. 27
DP AUG'57

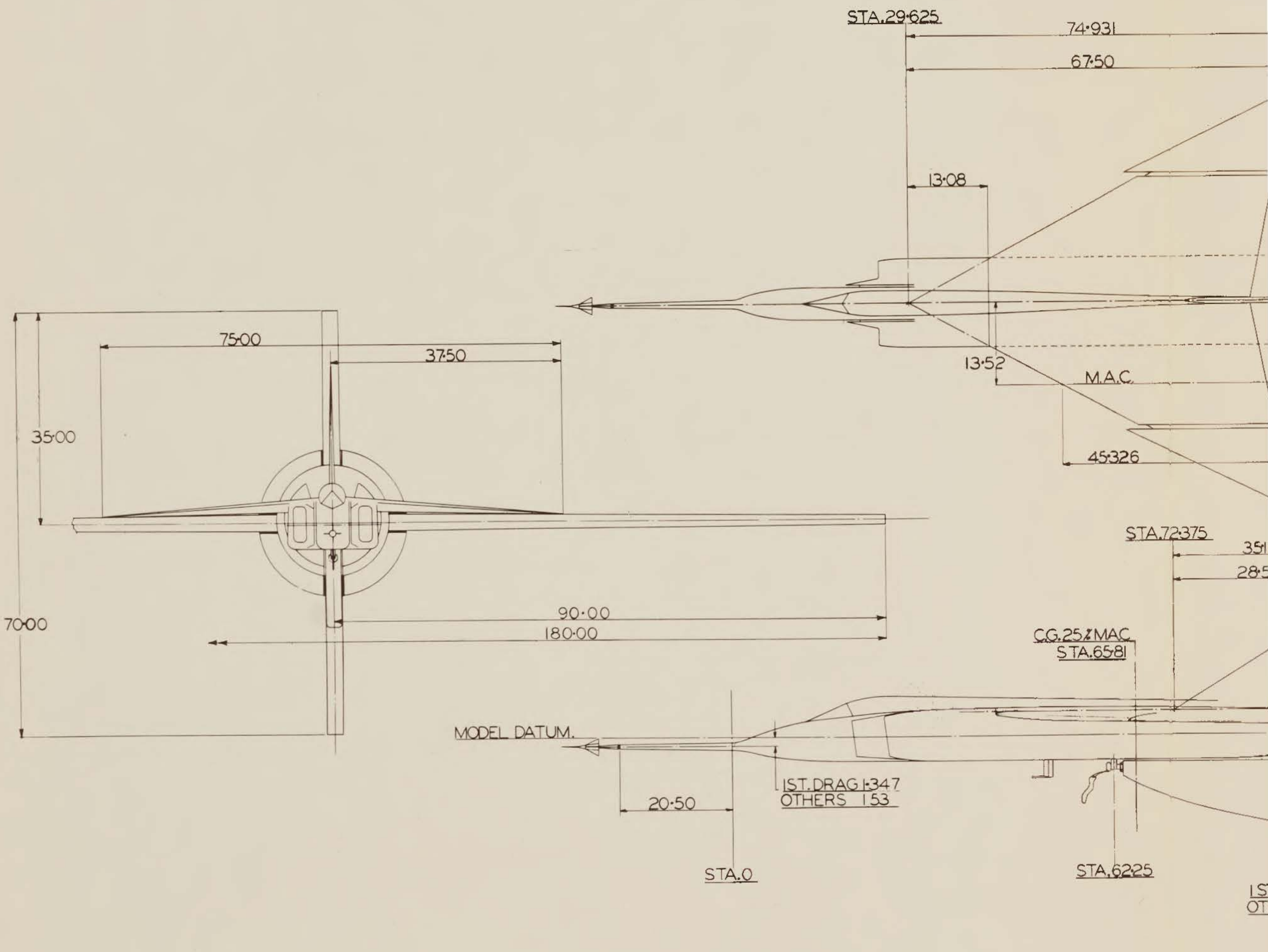
STA.29·625
74·931
67·50
13·08
13·52
M.A.C.
45·326
75·00
37·50
35·00
70·00
90·00
180·00
STA.72·375
C.G.25% MAC
STA.65·81
MODEL DATUM.
20·50
IST. DRAG 1·347
OTHERS 1·53
STA.0
STA.62·25

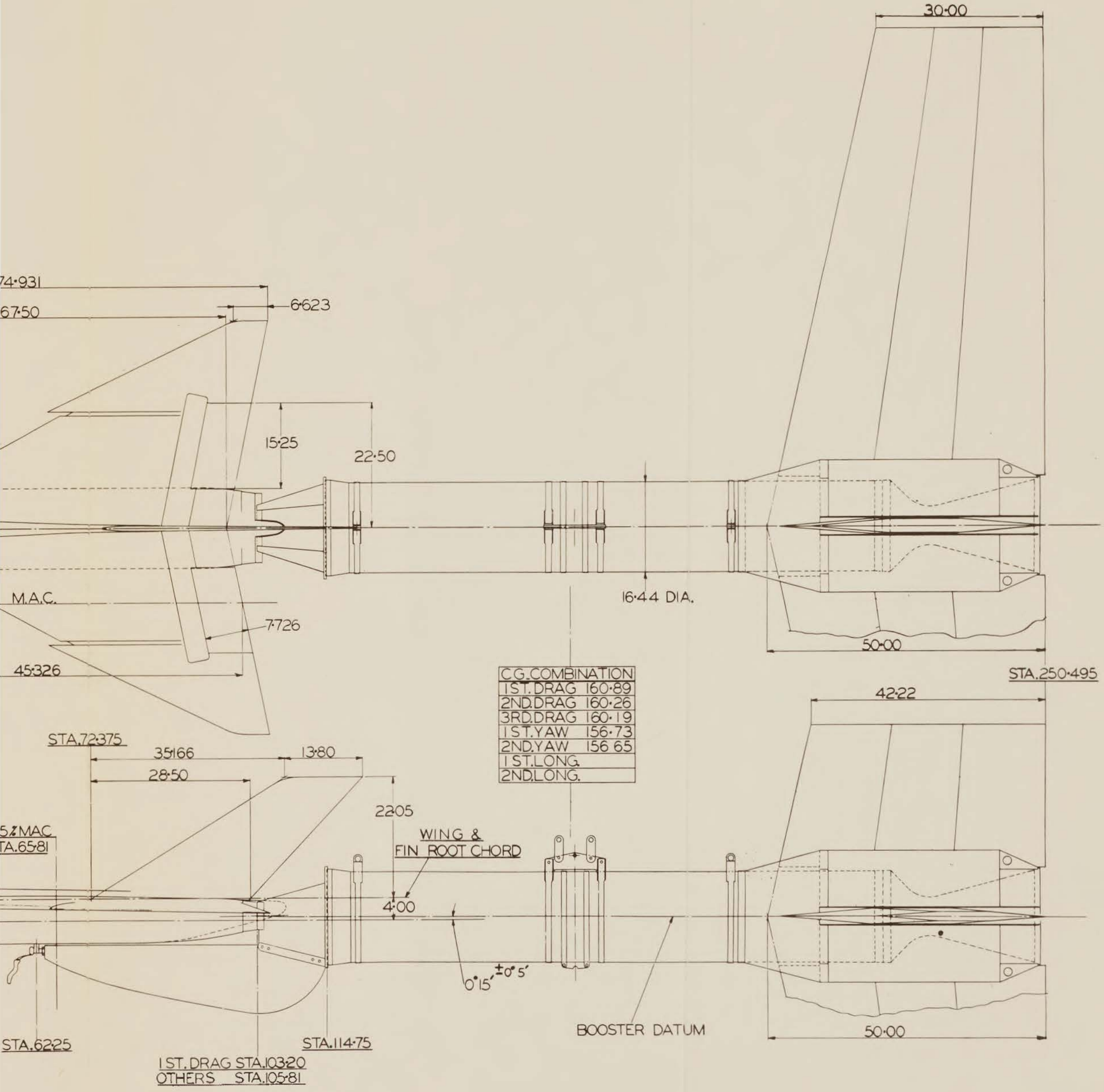

C.G. COMBINATION	
1ST. DRAG	160·89
2ND. DRAG	160·26
3RD. DRAG	160·19
1ST. YAW	156·73
2ND. YAW	156 65
1ST. LONG.	
2ND. LONG.	

FIG. 28

FIG. 30

DATE. MAR. 15-57
ISSUE. 1

P/GEOM/32 4

MODEL PROGRAM

C-105 AIRCRAFT

FREE FLIGHT MODEL Nº 6

DRAG MODEL Nº 2
FIRING DATE MAY 9-56
CONFIGURATION B_{3A} C_1 W_1 N_5 D_{8-4}
ELEVATOR LH 5°47' DWN
RH 5°36' "
MASS FLOW
INTAKE 5.6 FT^2
EXHAUST 7.068
THICKNESS RATIO
WING INNER 3.5 %
OUTER 3.5 T/J - 3.8 TIP

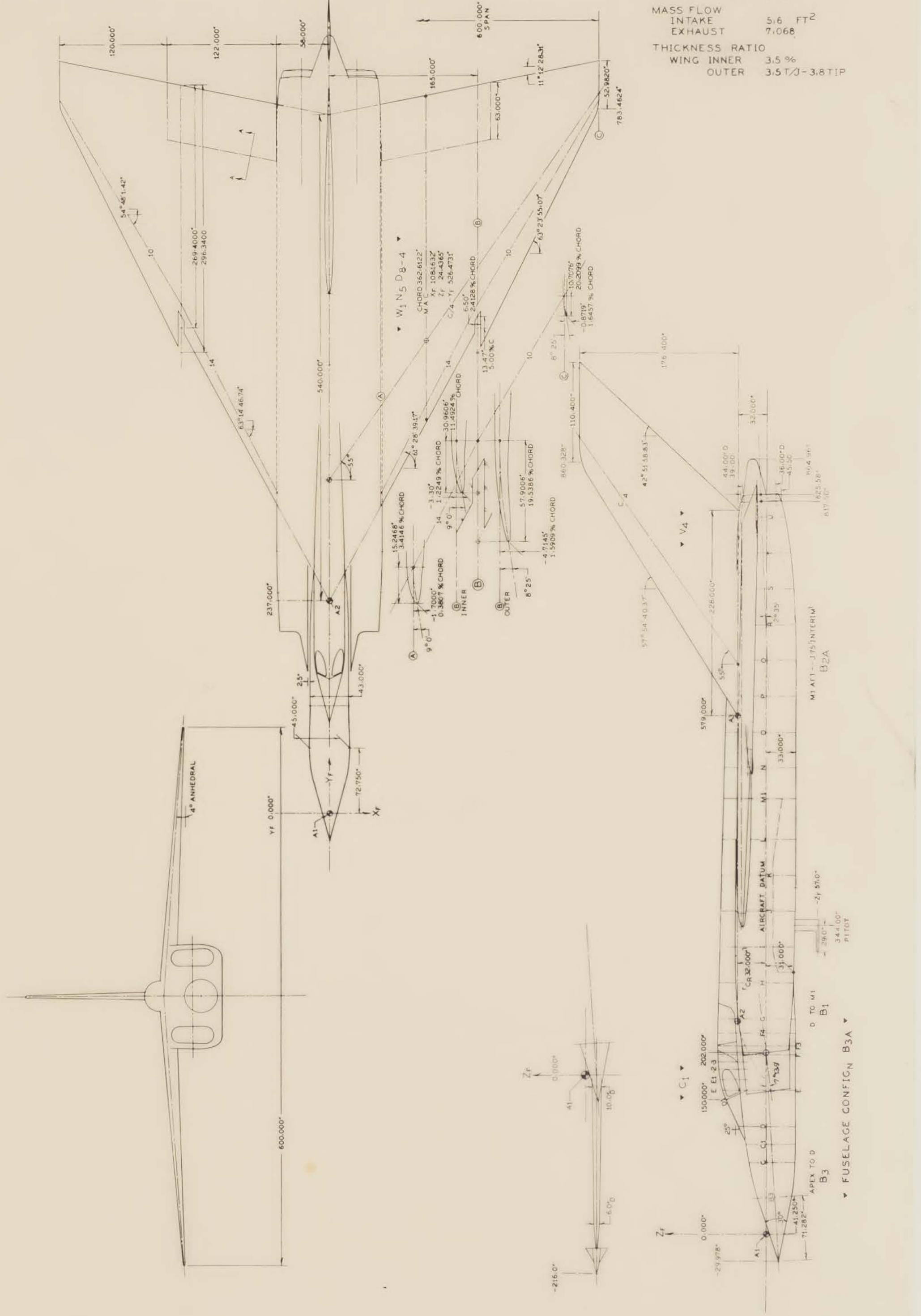

DATE APRIL 4-57
ISSUE 1

MODEL PROGRAM
C-105 AIRCRAFT
FREE FLIGHT MODEL Nº 7

DRAG MODEL Nº		3
FIRING DATE		MAY 15-56
CONFIGURATION		$B_{S4}\,C_{S4}\,W_1\,N_5\,D_{8-4}$
ELEVATOR	LH	5° 44' DWN
	RH	5° 38' "
MASS FLOW		
INTAKE		5.6 FT^2
EXHAUST		7.068 "
THICKNESS RATIO		
WING	INNER	3.5 %
	OUTER	3.5 T/J - 3.8 TIP
TAIL	ROOT	4.0
	TIP	3.8

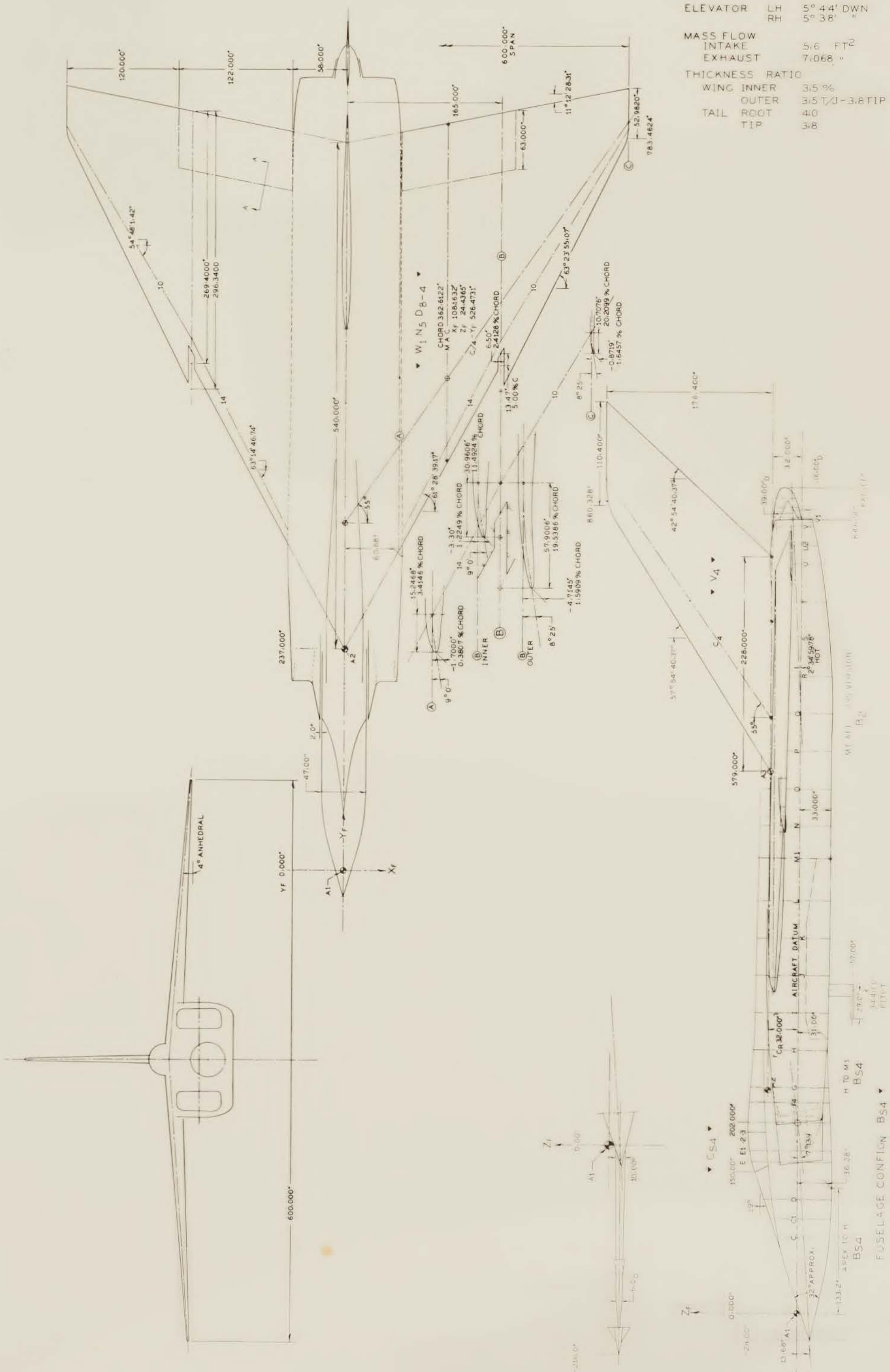

CONFIDENTIAL
UNCLASSIFIED

FIG.33
P/FFM/47
DLP AUG.'57

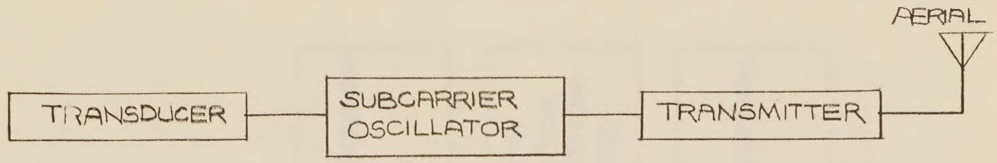

ELEMENTS OF AIRBORNE SYSTEM

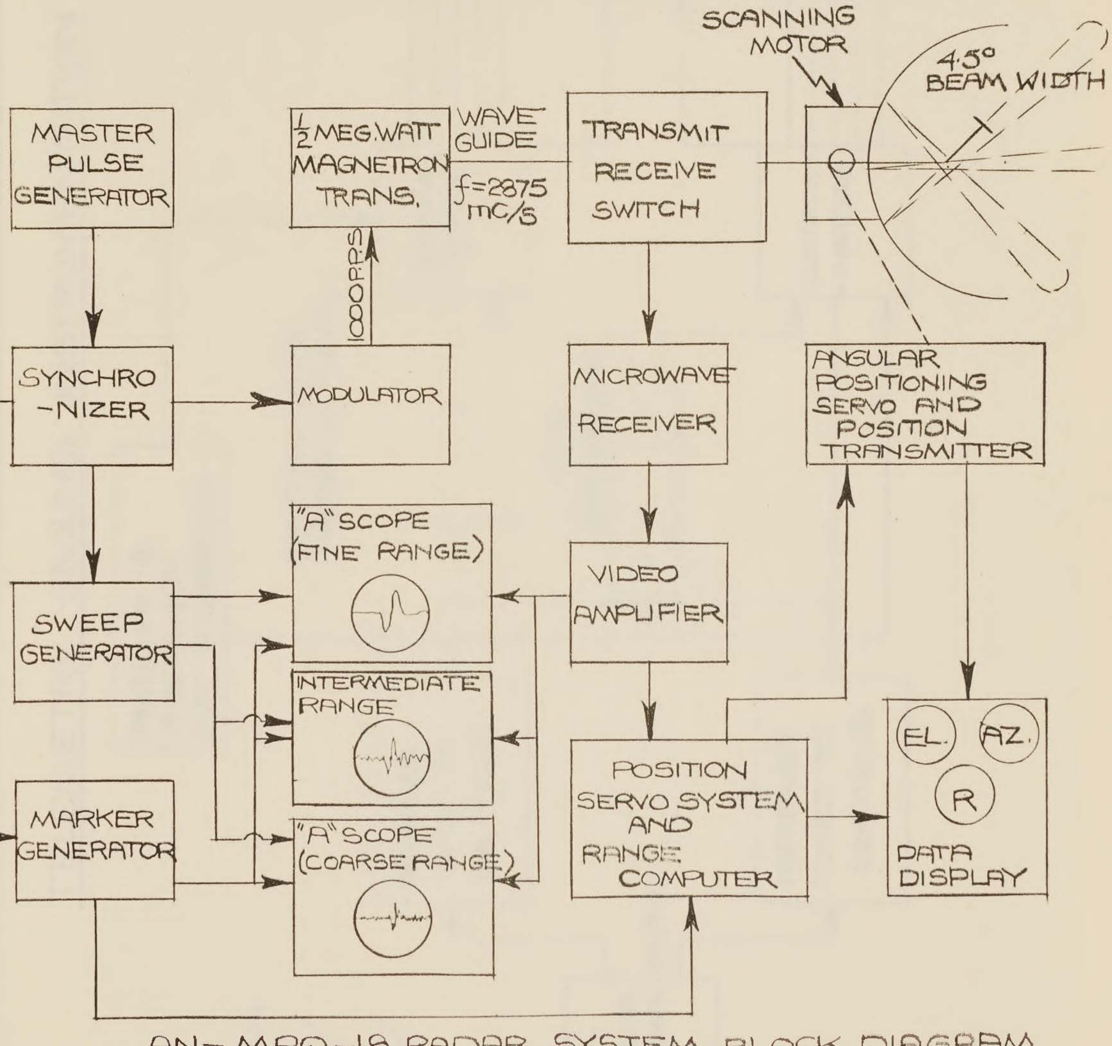

AN-MPQ-18 RADAR SYSTEM BLOCK DIAGRAM

TELEMETRY GROUND INSTRUMENTATION

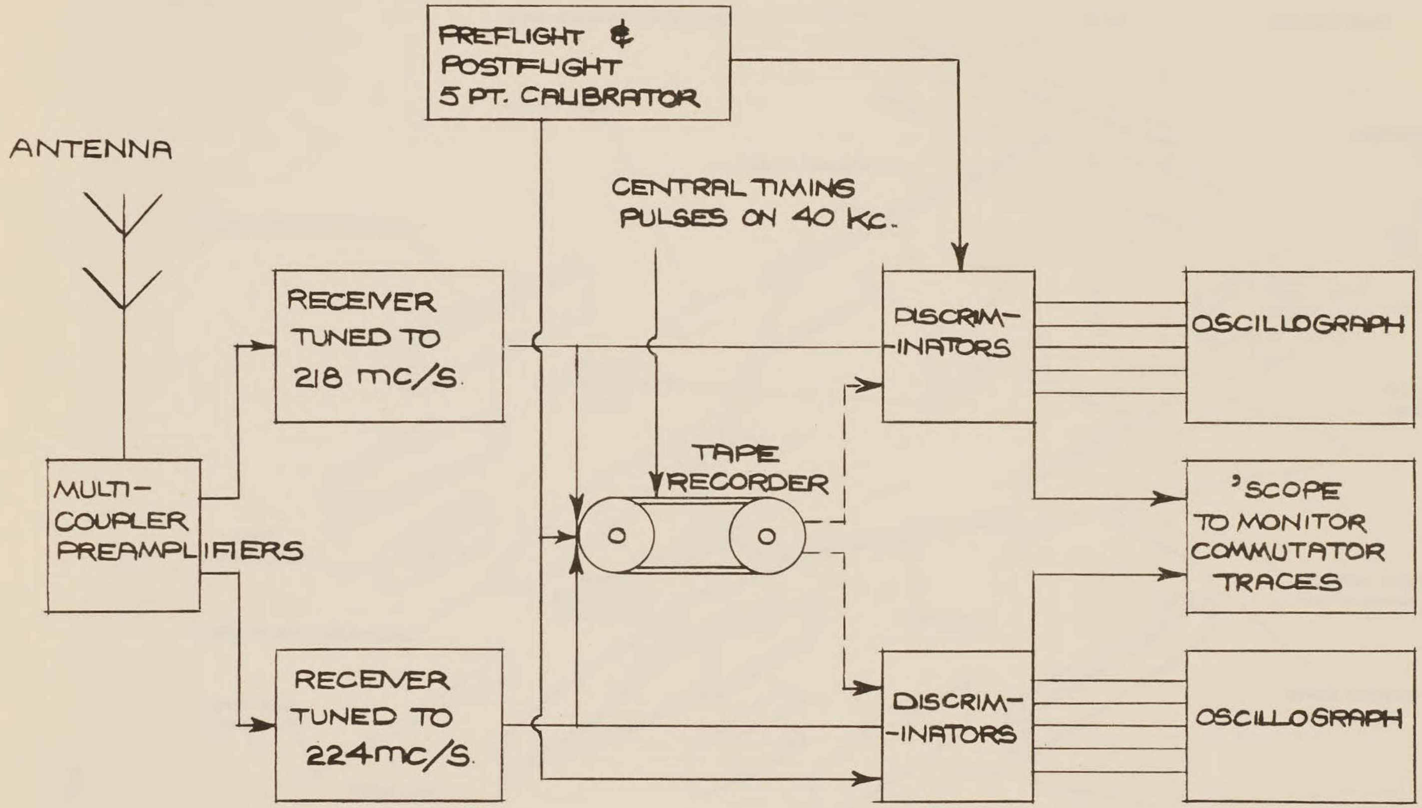

/CONT.

UNCLASSIFIED

P/FM/47 FIG.33
DP AUG.'57

2008-105-2

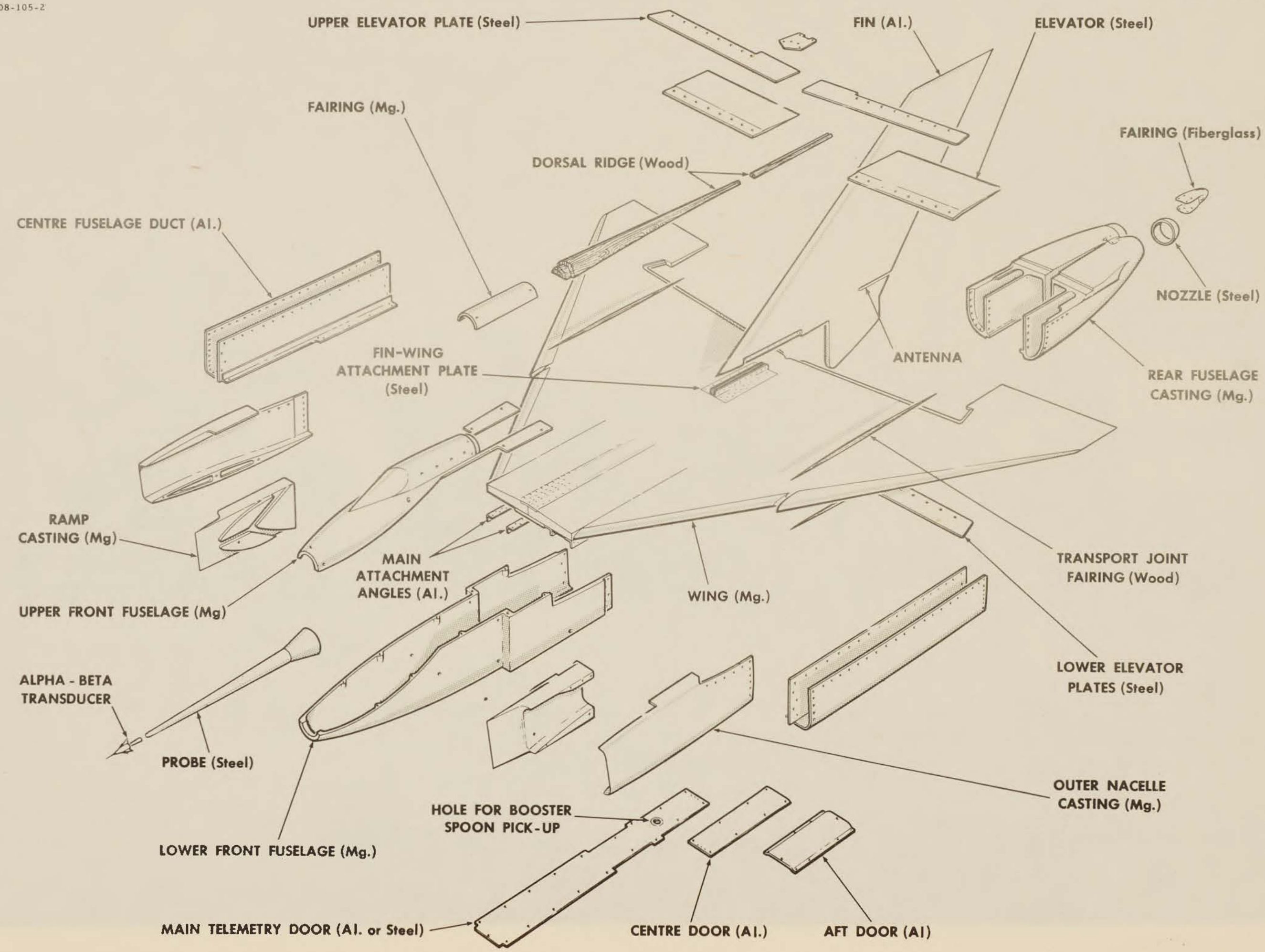

FIG. 34

CF-105 FREE FLIGHT MODEL-STRUCTURAL BREAKDOWN

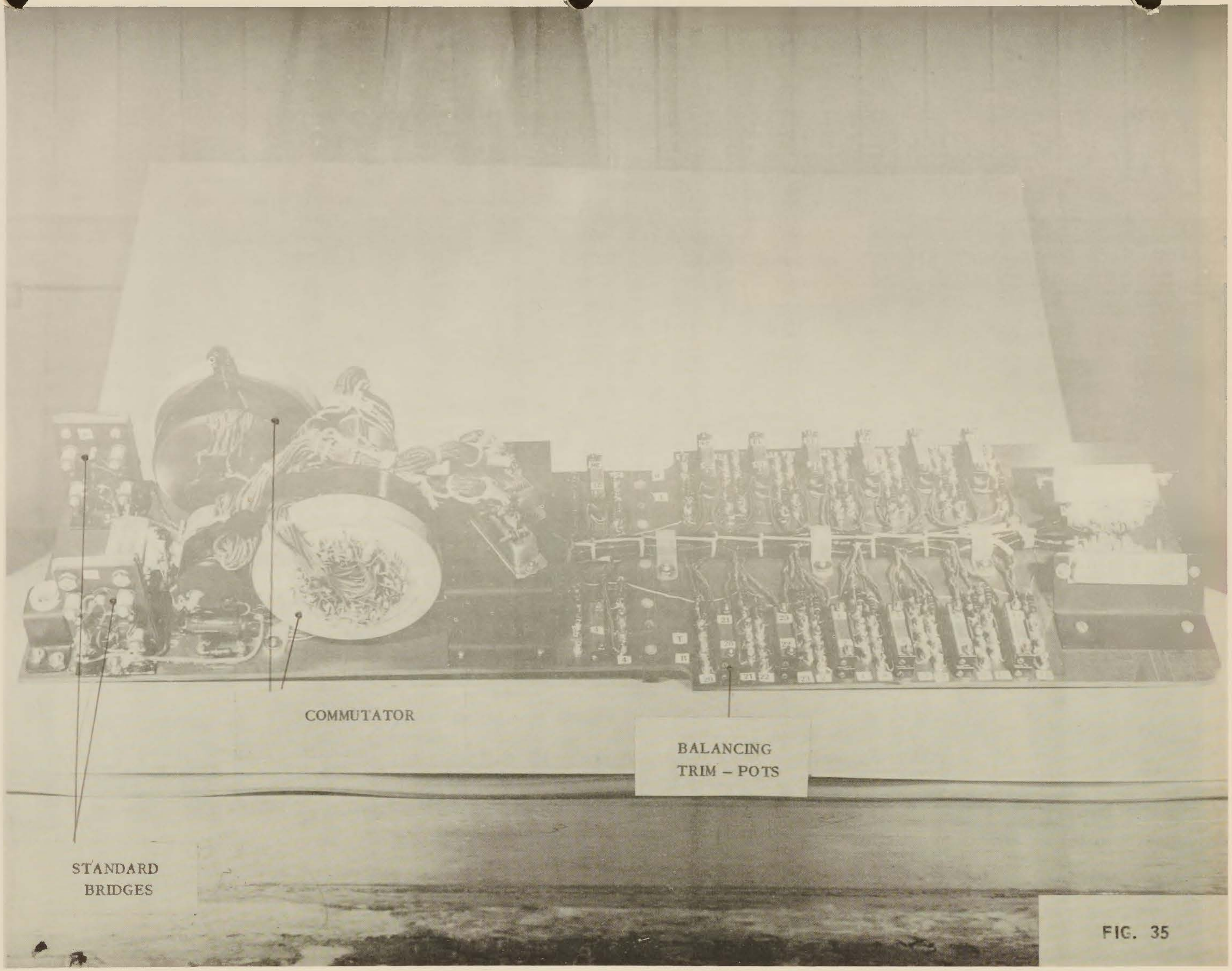

FIG. 35

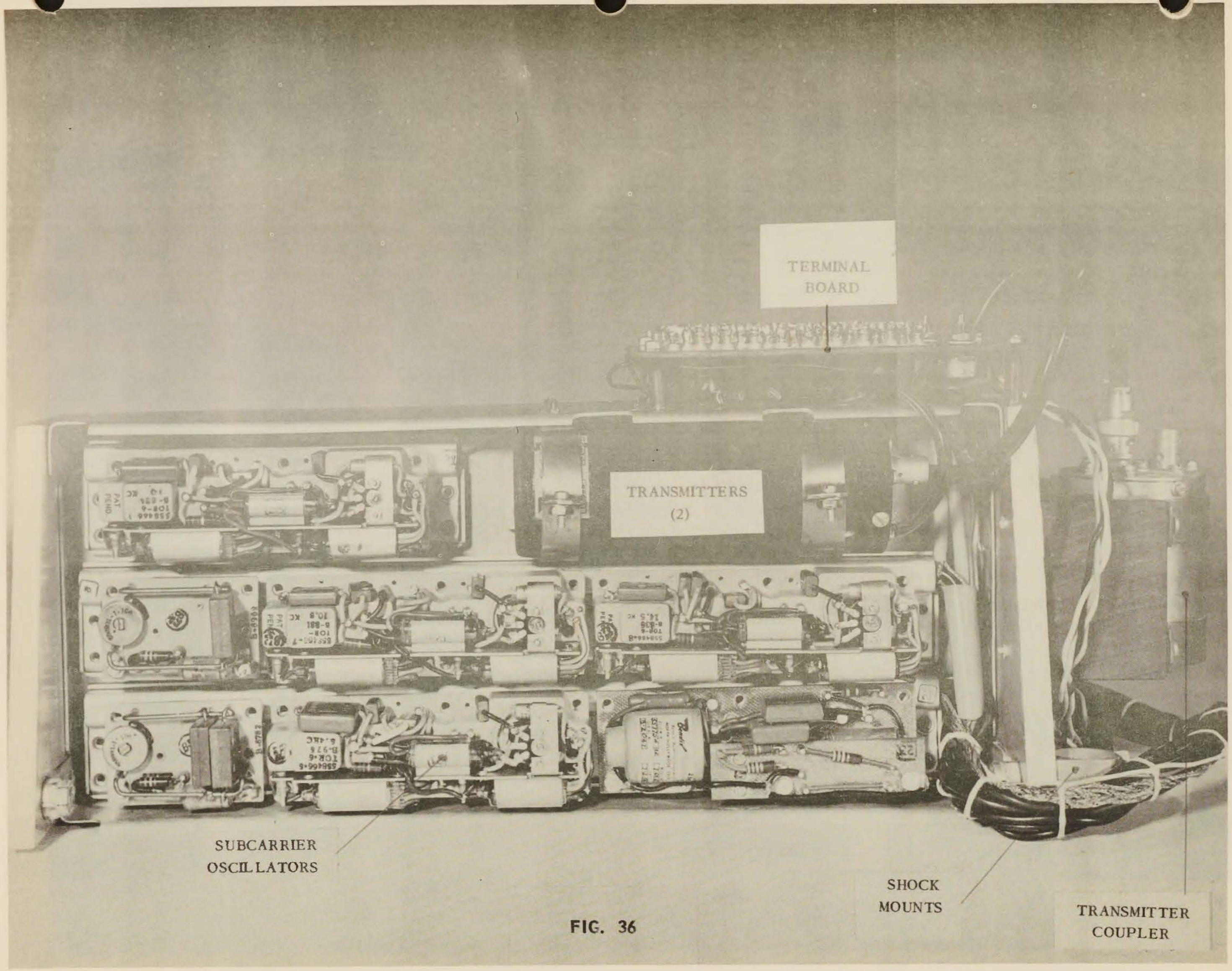
TERMINAL BOARD
TRANSMITTERS (2)
SUBCARRIER OSCILLATORS
SHOCK MOUNTS
TRANSMITTER COUPLER

FIG. 36

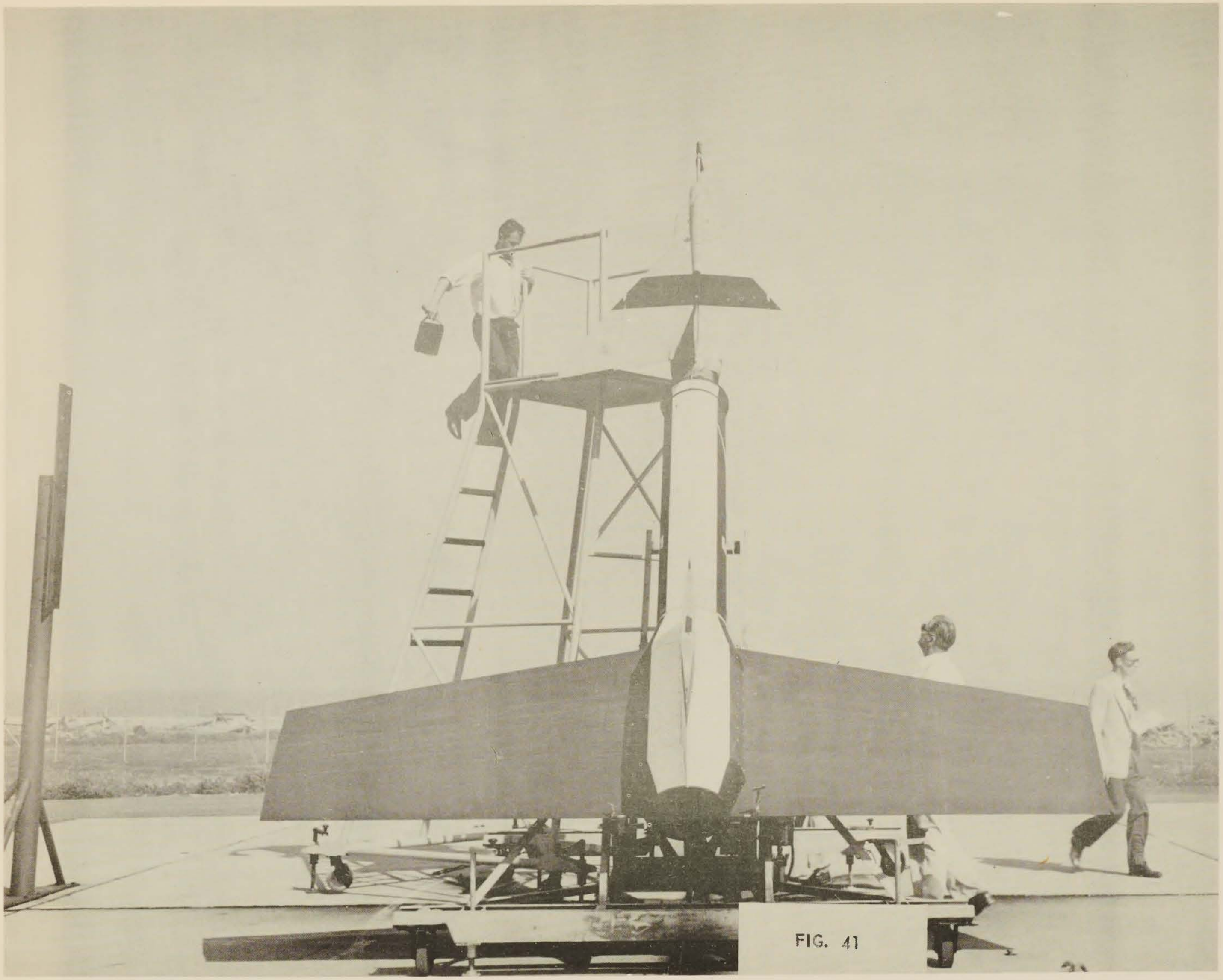

FIG. 41